Jesus Maria Blanco

INVESTIGATION OF TURBINE INTERACTIONS IN A TIDAL DEVICE.

SCHOOL OF ENGINEERING

MSc by Research

Cranfield UNIVERSITY

School of Engineering

Department of Power and Propulsion

MSc by Research

2009

J M Blanco

INVESTIGATION OF TURBINE INTERACTIONS IN A TIDAL DEVICE.

Supervisor: J. Amaral Teixeira

September 2009

ABSTRACT

Different tidal power generating systems have been studied for a long time. DeltaStream, which has been under development by Tidal Energy Limited has as a salient feature the fact that it is a tubular structure, equilateral triangle shaped and equipped with three horizontal axis turbines placed in each one of the vertices, fitted to nacelles that swivel as the tide flow reverses direction such as to present the rotor disc foremost to the incoming flow.

The main objective of this research is to evaluate the degree of angular mismatch that may occur between the turbines of this device as the nacelles are yawed onto a range of angular settings. The desired outcome is the maximisation of the power extractable by the whole system. In order to accomplish this, a numerical approach was carried out so a Computational Fluid Dynamics code FLUENT® v. 6.3 has been used.

The numerical model provides a faithful description of the support structure but initially, porous media discs are employed in order to represent the action of the turbine blades. A pressure loss is imposed, according to available data in order to obtain the wake created with the tidal stream. This basic model, considered adequate for an initial sizing of the problem, has been superseded by a realistic description of the blades. In a first stage, a frozen rotor scheme has been considered followed by the most realistic simulations counting the rotation of these blades. Results were finally compared with the previous ones and validated through an experimental prototype.

Due to the special character of the matter, which may lead indeed to innovative facts in the future, an extension of the subject would lead to improve results through grid adaptation (using velocity and/or pressure criteria) for all the models, but also with the study of the interferences when considering a further settling of a Delta farm.

ACKNOWLEDGEMENT

The author would like to thank Cranfield University, School of Engineering, especially to the Head of the Department of Power and Propulsion, Prof. Pericles Pilidis, for the chances given both before and during the project and also to the other members of the Staff for their friendly welcome and support during my stay.

I would also like to take the opportunity to give special acknowledgement to my supervisor Dr. Joao Amaral Teixeira, Lecturer at Cranfield University. The guidance and support he provided was very helpful for completing this work.

In addition the author would like to give many thanks to Mr. Richard Ayre, Senior Engineer from "Tidal Energy Limited" for his competent help providing all the information and experience to fulfil the project and also allowing the presentation of some of the results in an international conference in June this year.

Finally, a very special gratitude to Mr. Christopher Freeman, External Consultant of Cranfield University, and "alma mater" of this project, for his wise advice together with Dr. Florent Trarieux, from the off-shore group at Cranfield University, for providing experimental measurements to validate the CFD models.

Dedicated to my wife Elena and the children David and Andres.

TABLE OF CONTENTS

LIST OF FIGURES

LIST OF TABLES

LIST OF EQUATIONS

ABBREVIATIONS

BEM	Blade Element Momentum
BL	Boundary Layer
CAD	Computer Aided Design
CFD	Computation Fluid Dynamics
EMEC	European Marine Energy Centre
EP	European Union (patents office)
FEC	Finite Element Code
FSMCD	Flow Stream Momentum Conversion Device
HATT	Horizontal axis tidal turbine
IEA	International Energy Agency
LES	Large-Eddy Simulation
OENA	Off-shore Engineering and Naval Archicteture group
RNG	Re Normalization Group
SWF	Standard Wall Function
TEL	Tidal Energy Limited
TKE	Turbulent Kinetic Energy
UK	United Kingdom
US	United States of America
WO	World Organization (patents office)

NOMENCLATURE

A	Area of the rotor disc	m^2
A_W	Area affected by the wake of the upstream turbine	m^2
C	Constant (= 100) in equation 5.10	
C_{mg}	Constant (= 0.157) in equation 5.11	
C_2	Inertial resistance factor	m^{-1}
$c_f/2$	Friction coefficient	
Cv	Eddy-viscosity coefficient	
C_{PL}	Pressure Loss Coefficient	
D	Diameter of the disc	m
E	Energy extracted for the turbine in equation 4.1	W
E_{max}	Maximum power available to a turbine in equation 4.2	W
g	Acceleration due to gravitational forces	$m\ s^{-2}$
G_k	Generation of k due to the mean velocity gradients	
k	Turbulent kinetic energy term of the transport equation	$m^2\ s^2$
K	Permeability	m^2
$1/K$	Viscous resistance	m^{-2}
N_9	Number of 9 m. diameters (for the 9 m configuration)	
N_{10}	Number of 10 m. diameters (for the 10 m configuration)	
N_D	Number of diameters (for the Discrete blades configuration)	
P	Pressure	Pa
P_{AMB}	Ambient Pressure	Pa
P_D	Dynamic/Stagnation Pressure	Pa
PR	Pressure Ratio	
P_{STAT}	Static Pressure	Pa
P_{TOT}	Total Pressure	Pa
P_W	Pressure due to the wake of the upstream turbine	Pa
r	Radius	m
Re	Reynolds number	
RPM	Rotational Speed	rpm

S_i	Source term for the *ith* momentum equation.	
T_{STAT}	Static Temperature	K
T_{TOT}	Total Temperature	K
u_t	Friction velocity	m s^{-1}
U_{mean}	Mean fluid velocity	m s^{-1}
U	Velocity	m s^{-1}
U_0	Inlet Velocity	m s^{-1}
U_9	Velocity magnitude along the turbine axis (9 m)	m s^{-1}
U_{10}	Velocity magnitude along the turbine axis (10 m)	m s^{-1}
W	Mass Flow	kg s^{-1}
y_p	Size of the adjacent near- wall cell	mm
y_p^+	Adimensional sublayer thickness	

Greek symbols

α	Permeability factor	
Δp	Pressure drop per unit length	Pa m^{-1}
ε	Dissipation rate term of the transport equation	m^2 s^{-3}
ϕ	Porosity	%
ρ	Density of the seawater (1,025)	kg m^{-3}
μ	Dynamic viscosity of the fluid	kg m^{-1} s^{-1}
μ_t	Turbulent viscosity of the fluid	kg m^{-1} s^{-1}
μ_{eff}	Effective viscosity of fluid ($\mu + \mu_t$)	kg m^{-1} s^{-1}
υ	Kinematic viscosity	m^2 s^{-1}
η	Turbine efficiency in eq. 4.3	%
σ_k, σ_ε	Prandtl numbers for k and ε respectively	
τ	Torque	N m
Ω	Angular velocity of the turbine	Rad s^{-1}
γ	Yaw angle of the nacelles	Degrees
v_i	Velocity for the i th (x, y, or z) momentum equation	

1 INTRODUCTION

As renewable energy sources are becoming ever more and more important in the global energy scenario, the study focused on a device that seeks to exploit the marine sources such as marine currents, or tides as the means to generate power. The optimisation of tidal energy extraction devices is now a critical issue in order to increase efficiency when capturing maximum available energy in this aggressive sub sea environment.

When regarding the entire energy consumption of the world, the energy provided by renewable methods still represents in general terms a low proportion of the current needs [1, 2]. Figure 1.1 shows the world primary energy distribution according to the International Energy Agency (IEA), for the year 2008.

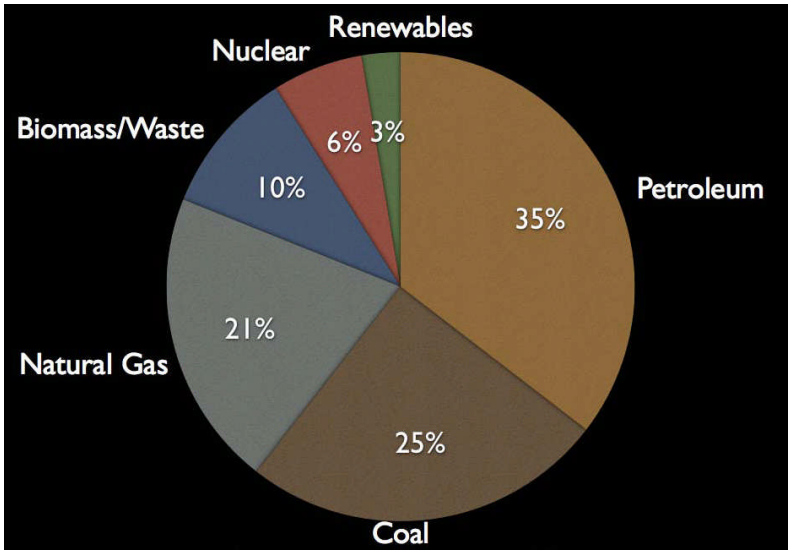

Source: International Energy Agency

Figure 1.1. World primary energy use in 2008.

The increasing usage of tidal power can improve this situation and hence reduce the reliance on CO_2 emitting technologies. However it is necessary to expand but also sustain the investment in research and development for this technology if the vision outlined above is going to become true [3, 4].

1.1 Tidal energy, origin and use

Tidal power is the only type of energy which comes directly from the relative motions of the Earth–Moon system, and to a lesser extent from the Earth–Sun system. The tidal forces produced by the Moon and Sun, in combination with Earth's rotation, are responsible for the generation of the tides.

A tide can be defined as the regular rise and fall of the surface of the ocean due to the gravitational force of the sun and moon on the earth and the centrifugal force produced by the rotation of the earth and moon about each other [5]. A bulge of water is created by the gravitational pull of the moon, which is greater on the side of the earth nearest the moon [6] as can be seen in Figure 1.2.

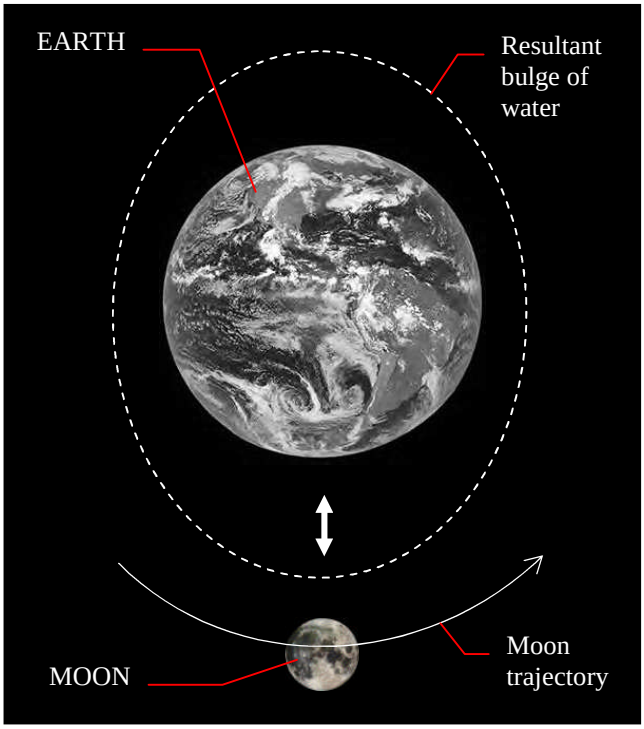

Figure 1.2. Tidal dynamics for earth and moon.

When a landmass lines up with this earth–moon system, the water around the landmass is at high tide and when the landmass is at 90º to the earth–moon system, the water around it is at low tide. Therefore, each landmass is exposed to two high tides and two low tides during each period of rotation of the earth [7, 8].

Since the moon rotates around the earth, the timing of these tides at any point on the earth will vary, occurring approximately 50 min later each day. Tidal currents are experienced in coastal areas and in places where the seabed forces the water to flow through narrow channels.

These currents flow in two directions; the current moving in the direction of the coast is known as the flood current and the current receding from the coast is known as the ebb current. The current speed in both directions varies from zero to a maximum. The zero current speed refers to the slack period, which occurs between the flood and ebb currents. The maximum current speed occurs halfway between the slack periods [9]. These tidal variations, both the rise and fall of the tide and the flood and ebb currents, can be utilised to generate electricity.

Tidal power is practically inexhaustible and can be classified as a renewable energy source, because the Earth's tides are caused by the tidal forces due to the combination of gravitational interaction with the Moon and Sun, and the Earth's rotation. A tidal energy generator uses this phenomenon to generate energy. The stronger the tide, either in water level height or tidal current velocities, the greater the potential for tidal energy generation [10].

Tidal movement causes a continual loss of mechanical energy in the Earth–Moon system due to pumping of water through the natural restrictions around coastlines, and due to viscous dissipation at the seabed and in turbulence. This loss of energy has caused the rotation of the Earth to slow in the 4.5 billion years since formation. During the last 620 million years the period of rotation has increased from 21.9 hours to 24 hours [11]. Tidal power can be classified in two main types [10]:

- Tidal stream systems make use of the kinetic energy of moving water to power turbines, in a similar way to windmills that use moving air, as can be seen in Figure 1.3.

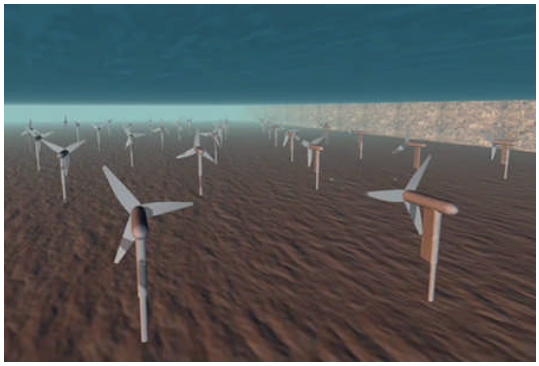

Source: Hammerfest Strϕm

Figure 1.3. Farm scheme of tidal turbines displayed on the seabed.

- Barrages make use of the potential energy in the difference in height between high and low tides. Barrages are essentially dams across the full width of a tidal estuary, and suffer from very high civil infrastructure costs, a worldwide shortage of viable sites, and environmental issues, as can be seen in Figure 1.4. Thus, the tidal barrage is a long-established, technically-proven concept which essentially involves a structure with gated sluices and low-head hydro turbines. This system has been in operation at "La Rance" on the northern French coast for more than 40 years. [12].

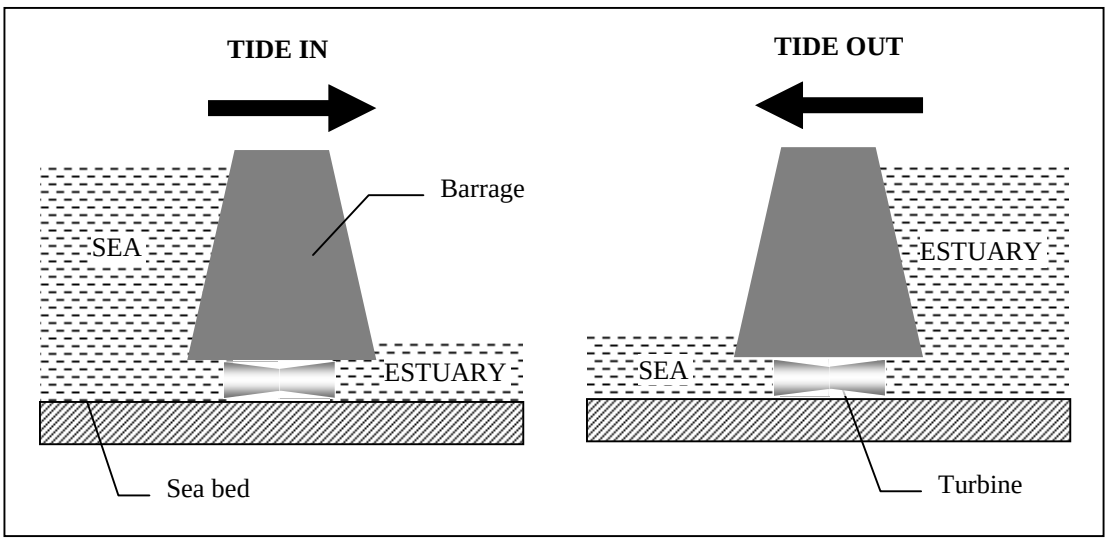

Adapted from: http://www.darvill.clara.net/altenerg/tidal.htm

Figure 1.4. Example of barrages working scheme.

Other configurations such as Tidal lagoons, can be considered similar to the barrages, consisting basically in closed structures. Most of the proposed tidal turbines resemble submerged wind turbines but there are also substantial differences in appearance stemming from the much larger structural loads these devices are subjected to [13].

Tidal stream turbines can be settled in areas where natural tidal current flows are concentrated such as numerous sites in Europe, but also south East Asia and Australia [10, 14]. Table 1.1 shows the Tidal potential of some large tidal range sites in Europe [15].

Some tidal sites can be considered bi-directional; however, some of them present flow reversal of 20 degrees or more away from 180 degrees such as the flow around islands, [16, 17]. This is for us the reason for chosing the maximum of 30 degrees yaw angle for the nacelles as will be shown later.

COUNTRY	CAPACITY (GW)
UK	25.2
France	22.8
Ireland	4.3
Holland	1.0
Germany	0.4
Spain	0.07
TOTAL	**63.8**

Table 1.1 Tidal potential of some large tidal range sites in Europe.

1.2 Context of the Project

The number of prototypes installed undersea for the last five years, has been increased notably, such as Marine Current Turbines' 300kW single rotor Sea flow device in Lynmouth (Devon, UK), from 2003. This company installed, early this year,

in Strangford Lough (Northern Ireland) its 1.2 MW Sea-Gen double rotor system [18], as can be seen in Figure 1.5.

Source: Marine Current Turbines.

Figure 1.5. SeaGen, the1.2 MW tidal energy generator installed in Strangford Lough.

DeltaStream, which has been under development by Tidal Energy Limited (TEL) since 2000 has as salient features the fact that it is freestanding, dispensing therefore the need for complex undersea foundations, and the fact that it combines three turbines in a single device. The DeltaStream configuration corresponds to a tubular structure, equilateral triangle shaped, which is placed in the sea floor and is equipped in the prototype configuration with three 300 kW turbines placed in each of the vertices of the delta, in order to extract the power of the submarine ocean currents [19].

The turbines are horizontal axis machines and are fitted to nacelles that swivel as the tide flow reverses direction such as to present the rotor disc foremost to the incoming tidal flow. The Department of Power and Propulsion of Cranfield University and TEL, joined a research programme focused on this device so this project was situated inside this context.

1.3 CFD Implementation

Computational Fluid Dynamics (CFD), solve equations implemented to define the physics of fluid flow through numerical methods, so it has been revealed as a

powerful tool which can provide detailed information about the local flow and hence performance of a marine current turbine [10, 20]. Cranfield University has license for several CFD codes such as CFX, FLUENT, etc. For this work, the latest version of the code FLUENT® v. 6.3 has been used whilst the computational meshes were assembled in GAMBIT® v. 2.4.

Initially, discs are employed in order to represent the action of the turbine blades. The discs consist of a porous media though which a pressure loss is imposed, according to available data. A seventh power law inlet velocity profile is employed. As these marine currents are in constant movement both in angle and magnitude, the disc of the turbines must be also rotating all the time in order to face them and reach this way the maximum efficiency, so for example, when two turbines are aligned, the wakes created will cause problems to the turbine situated right downstream because of the pressure drop. Several cases have been performed here in order to evaluate the interferences between the three marine turbines. Thus, a range from 0 to 30 degrees was analysed, considering successive intervals of 5 degrees.

This simplistic model was considered adequate for an initial sizing of the problem but has been superseded by a more realistic description of the turbines, including discrete blade representations whose results will be presented later. In a first stage, a frozen rotor scheme has been considered in order to predict the behaviour of the flow around the blades and the subsequent effect to the other turbines of the delta configuration with a reasonable computational effort and finally the most realistic simulations were carried out, implementing the rotation of these blades according to available data.

A validation process was carried out first of all with experimental data obtained through a 1/30 scale model tested in a water tank, showing good agreement with the results offered with the CFD models in terms of velocity profiles measured at different locations both upstream and downstream of the delta. A second way of validation for the CFD models were the results obtained from the literature, showing all of them good

agreement with the results offered with the CFD models, so these models were considered validated.

2 AIMS & OBJECTIVES

2.1 Aim of the Thesis

The aim of this work is to provide a computational model for a faithful description of the flow through this particular DeltaStream device. This study complements the DeltaStream development work carried out in the Department which focussed primarily on a single turbine.

2.2 Objectives

The main objective of this research is to evaluate the degree of interference that may occur between the turbines of this marine device as the nacelles are yawed onto a range of angular settings (from 0 to 30 degrees). The desired outcome is the maximisation of the power extractable by the whole system. For this, a commercial CFD package called FLUENT® has been used. Several models have been developed in order to simulate the effect that these turbines induce on the flow but also on the other turbines of this particular device.

The CFD study will permit the identification of the range of angular mismatch that non-reciprocating tides, which are observable in particular locations, can induce on these marine devices.

Through the results achieved in this project, the author is expected to provide a set of recommendations in order to evaluate the wake interactions induced for the whole device that would lead to improve efficiency.

3 PROJECT MANAGEMENT

3.1 Methodology

As a CFD based study, discs were employed for the earliest stages of this work in order to represent the action of the turbine blades on the flow. The discs consisted of a porous media through which a pressure loss is imposed, according to available data related to real devices. A comparative testing of 9 and 10m diameters discs was studied for a complete range of angular rotation for the nacelles from 0-30 degrees. This angle range was considered sufficient to deal with mismatch between the tidal stream flowing in the two, outgoing and incoming, directions.

A more realistic definition of the delta device was considered subsequently, in order to include discrete blade representations for each of the three turbines. Initially a steady study was performed with the blades and nacelles at different rotational angles. This study was not finally presented here as results were considered not enough relevant. After that, a frozen rotor configuration (called “Moving Reference Frame” in FLUENT®) was employed and finally a full transient model (called “Moving Mesh” in FLUENT®), being the most complex and computationally costly model, was used in the simulations. This model was applied to the same range of turbine yaw angles as mentioned above.

CFD results from the latter models were carefully compared with those from the porous media models and validated finally through a 1/30 scaled experimental prototype tested towards the end of the project in the water tank of a research centre in France. The comparisons showed in general good agreement, particularly after some improvements were performed for the CFD models, especially for the latest ones, considering in this way the SST k- ω turbulence model as the best approach, instead of the initial k-ε (REALIZABLE).

3.2 Project Planning

The project has been structured basically in eight phases:

Phase 1. Aims and methodology.

The first phase deals with the establishment of the objectives and the most appropriate methodology for the project to be fulfilled both in time and objectives. Several meetings both with the supervisor but also with the delegates of the sponsor company were necessary. About four weeks were considered enough to complete this phase.

Phase 2. Literature review.

This phase mainly covers a complete search of the state of the art regarding tidal devices, such as published papers in some of the most important journals, relevant conferences, recent patens, web sources, etc. Also a brief description of the background theory regarding the energy extraction from tides and covering the most important marine turbine strategies including the evolution of the concept was considered here. This phase overlaps the previous one, so both activities were carried out at the same time.

Phase 3. The porous media model.

After the literature review was partially completed, the building of the first computational model was started. This was the so called “porous media model” because the effect of the blades was simulated through porous discs as a first approach to the problem, considering that two different diameters for the discs (9 and 10 m respectively) as well as several rotational angles both for the nacelles and discs (0-30 degrees) were performed.

Phase 4. Analysis of partial results.

Once the first model was created, the results directly achieved with the porous models were analysed in dept. It permitted the identification of the range of angular mismatch that tides can induce on this particular configuration of marine device when the three nacelles are yawed onto the above mentioned range of angular settings

inducing a significant velocity drop to the incoming flow towards the downstream turbines. For this, several cases were analysed, and results were watchfully presented every 5 degrees of angular rotation for both nacelles and discs.

Phase 5. The frozen rotor model.

This second model was started fully overlapping the previous phase, where a more realistic profile for the blades was implemented according to available data and performed in a non-stationary way. The complexity of the meshing process must be highlighted, particularly regarding the blades. Further improvements of the grid were required in order to be able to capture the small scales of turbulence around these areas through a deep mesh refinement according to high pressure gradients.

Phase 6. The rotating blades model.

Finally the more complex model was performed, overlapping partially the previous phase, so the non-stationary detailed study of the rotating blades was taken into account. A huge computational effort was required for the convergence to be reached.

Phase 7. Validation of the models.

Through experimental data, based mainly on experimental velocity measurements over a 1/30 scale model in a water tank, carried out by the Off-shore Engineering and Naval Archicteture (OENA) Group of Cranfield University the validation of the models was successfully carried out.

Phase 8. Conclusions.

With all of the information reached in this study, future recommendations were provided considering that the main objective was the maximisation of the power extractable by the whole device. In this work a characterization of the behaviour of the flow over a particular marine device under different situations has been studied highlighting the degree of angular mismatch that may occur between the turbines of this device as the nacelles are yawed onto a range of angular settings.

4 STATE OF THE ART

This chapter describes basically the fundamental background theory and also highlights the most significant work done in this field, for the last few years, considering various types of techniques which are currently used in industry to extract power from the tides [19, 20]. It shows mainly the evolution of the horizontal axis turbines, which have the bigger number of prototypes currently operating, such as the one studied in this work.

A comprehensive review of the state of the art has been carried out in terms of tidal turbines design and optimization. The author was invited by the editor of an international journal, to write a review paper regarding recent patents in the field of tidal turbines. This was finally published after the corresponding peer review process [21].

Finally, part of this work, corresponding to the results achieved with the porous media models, were presented to an international conference in Barcelona (Spain) in June 2009, regarding Numerical Methods in Engineering [22].

4.1 Background theory

The energy that can be extracted from the tides is due to movements of water in the sea. On one hand the movement of the tides is flow and ebb, water is continuously raised and lowered so this potential energy can be obtained. On the other hand the energy extracted from the waves is due to movements of water near the surface of the sea [22].

It must be pointed out that wind generated waves are formed by winds blowing over the water surface, so the water particles adopt turbulent motion and the kinetic energy can be obtained. The amount of this energy is determined by several aspects

such as the speed and duration of the wind, the length of sea it blows over, the water depth, sea bed conditions and also interactions with the tides [23].

The physics of the conversion of energy from tidal currents is superficially very similar, in principle, to the conversion of kinetic energy from the wind through the use of wind turbines. The environment that a tidal device operates in is substantially different from that experienced by a wind turbine. “The higher density of water, 832 times the density of air, means that a single generator can provide significant power at low tidal flow velocities (compared with wind speed). Given that power varies with the density of medium and the cube of velocity, it is easy to see that water speeds of nearly one-tenth of the speed of wind provide the same power for the same size of turbine system” [24].

4.1.1 *Tidal power extraction strategies*

A large number of devices have been proposed for the extraction and conversion of tidal energy to electricity. Nowadays three types of device suitable to capture tidal stream energy can be highlighted [12]:

- *Tidal stream turbines*. These work on a similar principle to wind turbines and indeed may have a quite similar external appearance. Both horizontal and vertical axis machines are being under research programs, some with ducting/cowling around the rotor. The turbine may be coupled directly to a standard generator via a gearbox, or use an alternative power train design.

- *Reciprocating tidal stream devices*. These have hydrofoils which move back and forth in a plane normal to the tidal stream, instead of rotating blades. A particular design uses hydraulic pistons to feed a hydraulic circuit, which turns a hydraulic motor and generator to finally produce power as can be seen in Figure 4.1.

Source: Engineering Business

Figure 4.1. The 150 kW reciprocating "Stingray" tidal generator.

- *Venturi effect tidal stream devices*. In these, the tidal flow is directed through a duct, which concentrates the flow and produces a pressure difference.

Tidal power can also be extracted from other configurations such as tidal barrages and tidal lagoons as has been previously commented in the introduction section although this is supported by another slightly different technology.

4.1.2 *Evolution of the horizontal axis machines*

These turbines are close in concept to traditional windmills but operate under the sea and have the biggest number of prototypes currently operating. The evolution of these machines along the last few years is presented next [25].

- "Kvalsund, south of Hammerfest, Norway, a turbine with a reported capacity of 300 kW was connected to the grid on 13th of November 2003.

- A 300 kW marine current turbine, Seaflow, was installed by Marine Current Turbines off the coast of Lynmouth, Devon, England, in 2003. The 11m diameter turbine generator was fitted to a steel pile which was driven into the seabed. As a prototype, it was connected to a dump load, not to the grid.

- Verdant Power has been running a prototype project in the East River between Queens and Roosevelt Island in New York City since April 2007. It was the first major tidal-power project in the United States.

- SeaGen, was installed by Marine Current Turbines in Strangford Lough in Northern Ireland in April 2008 [26]. The turbine began to generate around 150 kW into the grid for the first time on the 17th of July 2008. The initial set of blades suffered some damage and new reinforced blades were installed in September 2008. Finally, the turbine began to generate at full power, about 1.2 MW, in December 2008. It is currently the only commercial scale device to have been installed anywhere in the world.

- OpenHydro", an Irish company exploiting the Open-Centre Turbine developed in the U.S., has a prototype being tested at the European Marine Energy Centre (EMEC), in Orkney, Scotland [27, 28] as can be seen in Figure 4.2.

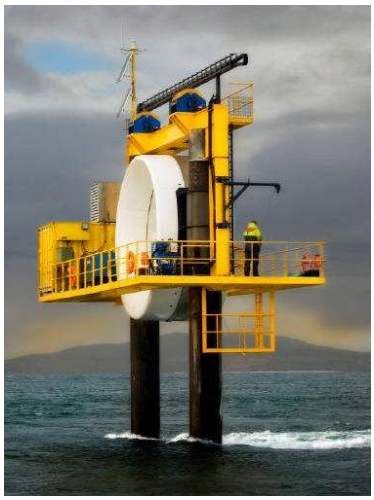

Figure 4.2. OpenHydro's turbine research facility at the EMEC in Orkney, Scotland.

Table 4.1 shows a list with the most important US and European Tidal Energy Developers, together with the technology used.

COMPANY	TECHNOLOGY	COUNTRY
Aquamarine Power	Neptune	UK
Edinburgh Designs	Vertical-axis, variable pitch tidal turbine	UK
Edinburgh University	Polo	UK
Greenheat Systems Ltd	Gentec Venturi	UK
Hydro Green Energy	Hydrokinetic Turbine	USA
Hydro-Gen	Hydro-gen	France
Hydrohelix Energies	hydro-helix	France
Hydroventuri	Rochester Venturi	UK
Kinetic Energy Systems	Hydrokinetic Generator, KESC	USA
Lunar Energy	Rotech Tidal Turbine	UK
Marine Current Turbines	Seagen, Seaflow	UK
Natural Currents	Red Hawk	USA
Neo-Aerodynamic Ltd Company	Neo-Aerodynamic	USA
Neptune Renewable Energy Ltd	Proteus	UK
Ocean Flow Energy	Evopod	UK
Ocean Renewable Power Company	OCGen	USA
Oceana Energy Company	TIDES	USA
OpenHydro	Open Centre Turbine	Ireland
Ponte di Archimede	Kobold Turbine	Italy
Pulse Generation	Pulse Generators	UK
Scotrenewables	SRTT (Scotrenewables Tidal Turbine)	UK
SMD Hydrovision	TiDEL	UK
Swanturbines Ltd.	Swan Turbine	UK
The Engineering Buisiness	Stingray	UK
Tidal Electric	Tidal Lagoons	UK/USA
Tidal Generation Limited	Deep-gen	UK
Tidal Hydraulic Generators Ltd	Tidal Hydraulic Generators	UK
TidalStream	TidalStream	UK
University of Southampton	Southampton Integrated Tidal Generator	UK
University of Strathclyde	Contra-rotating marine current turbine	UK
Verdant Power	Various	USA
Water Wall Turbine	WWTurbine	USA

Table 4.1. List of the most important US and European Tidal Energy Developers.

4.1.3 *Basic energy calculations*

Different overall efficiencies can be achieved from these previously shown strategies and therefore different power outputs can be obtained. The equation below can be used to determine the power that can be extracted from one of these devices or the so called power output [20]:

$$E = \tau \cdot \Omega \qquad \textbf{Equation 4.1}$$

where E is the power of the turbine, τ is the torque and Ω is the rotational speed.

The maximum power available to a turbine (E_{max}), is the kinetic energy of the fluid in a stream tube whose diameter, at the turbine disk plane, is equal to the diameter of the turbine as can be seen in the equation below.

$$E_{\max} = \frac{1}{2} \cdot \rho \cdot A \cdot U_{mean}^{3} \qquad \textbf{Equation 4.2}$$

where ρ is the density, A is the area of the disk and U_{mean} is the mean fluid velocity. This allows the efficiency of the turbine, to be defined as a percentage as:

$$\eta = 100 \cdot \frac{E}{E_{\max}} \qquad \textbf{Equation 4.3}$$

A problem may arise when these devices are placed in close proximity. Then additional interference can be caused over the closer devices in terms of pressure drop, which means significant fluctuations of the efficiency.

Taking into account that these turbines are horizontal axis machines and are fitted to nacelles that swivel as the tide flow reverses direction, such as to present the rotor foremost to the incoming tidal flow, a range of angular positions of the nacelles needs to be carefully examined with the tidal stream flowing in the two, outgoing and incoming, tidal directions [29 - 31]. The analysis of these results will allow a qualitative

identification of the range of angular mismatch induced and the subsequent effect on the efficiency of the overall set of turbines.

4.2 Literature review

A summarized review including papers, posters and conferences recently published (some of them have already been referenced in this work so the number of its reference has also been included), are commented next, followed by a list of recent patents, in order to highlight the most relevant advances reached nowadays in current turbines design and optimization, in terms of power output and improving efficiency.

4.2.1 *Papers*

Nicholls-Lee, 2008, [10] suggested that an increase in performance can be obtained by means of variable pitch blades and that other materials can be utilised in the design of tidal turbine blades. Another relevant comment is that many tidal sites have relatively bidirectional flow. However, some sites may have flow reversal of over 20 degrees from 180 degrees such as the flow around islands and headlands. This assumption has been considered relevant in the work developed for this thesis.

Nicholls-Lee et al, 2008, [16] deals with the methods of simulation based optimisation for marine current turbines. BEM and CFD codes together with Finite Element analyses are referred in this manuscript. The significance of design, search and optimisation with respect to complex fluid and structural modelling is also discussed.

Egarr et al, 2004, [20] modelled a tidal turbine using CFD which was validated against experimental data. This is the first stage in the process of optimising a turbine to extract energy from the tide. The redevelopment of the flow downstream from the turbine has also been studied. This approach has been of a great importance for us. This work clearly indicates the feasibility of the CFD study for tidal turbines design, in order to maximize the extraction of energy from the tides.

Germain et al, 2007, [28] provides useful information for the hydrodynamic characterization of marine energy converter systems, their design and validation, including the procedure for the characterisation of the wake of horizontal axis marine current turbines which has been of a great interest together with the next contribution.

Bahaj et al, 2007, [30] presents a discussion on the characterisation of the wake of horizontal axis marine current turbines. An experimental and theoretical investigation of the flow field around small-scale mesh disc rotor simulators is presented and wake characteristics of the rotor simulators were reported.

Karsten et al, 2008, [31], examined the tidal power available for electricity generation from stream turbines placed in a particular location. This suggests that the greatest tidal power will be possible in channels where the product of the flowrate through the channel and the tidal amplitude at the entrance of the channel is large, so it can be deduced that its application under the sea is completely suitable.

Nicholls-Lee, 2007, explained how through the use of fluid-structure interactions modelled computationally using CFD, but also through practical testing in towing tanks and open water, adaptive materials could be integrated into tidal turbine blade design in order to increase its efficiency.

Whelan et al, 2007, presented some relevant theoretical results for the case of a linear array of tidal stream turbines. These results were compared to open channel flow experimental results as also performed by [32]. The flow field was experimentally simulated using various resistance discs accordingly to [33, 34].

Vafai et al, 1981, [35], focused their study on the inertial forces on flow and heat transfer in porous media. A numerical proposal for the governing equations has been implemented here in order to investigate the velocity and temperature fields inside a porous medium, and a new conception of the momentum boundary layer has also been presented.

4.2.2 *Patents*

A comprehensive review, regarding the state of the art has been carried out in terms of tidal turbines design and optimization techniques. A summary list with the most relevant US, WO and EP patents has been assembled and is shown, including a brief description of each issue. The more relevant topics for the search were: “Tidal streams, Marine Current Turbines, Reciprocating tides, Blade interferences, kinetic energy from tides, single/double rotor Systems, etc…”. The next search engines have been used:

- “http://www.uspto.gov”
- “http://ep.espacenet.com”
- “http://www.freepatentsonline.com”
- “http://www.google.com/patents”
- “http://patft.uspto.gov/netahtml/PTO/search-bool.html”

A list of the most relevant WO (international) patens have been summarised in Table 4.2 [36-40] while Table 4.3 shows the same for EP (european) patents [41-45] and finally, US patents summary list is showed next, also in chronological order in Table 4.4 [46-54], including in all of them a brief description of the issue.

Technologies involved in tidal devices can be categorised into two main types: tidal barrages and tidal current turbines. A brief summary of these technologies will be shown next.

Tidal barrages make use of the potential energy of the tides. It is typically a dam, built across a bay or estuary. Electricity generation from tidal barrages employs the same principles as hydroelectric generation, except that tidal currents flow in both directions. A typical tidal barrage consists of turbines, sluice gates, embankments and shiplocks.

Number	Date	Description
WO2003025385	2003	"This invention provides a bi-directional turbine with dual counter-rotating rotor disks to create a stable, efficient turbine generator unit minimizing swirl losses".
WO2005078276	2005	"Presents a power buoy for a tidal turbine installation which is an alternative to the conventional manner of generating power in river power stations, particularly in all those surroundings requiring high lateral, tight dams in addition to the barrage for damming up".
WO2007125538	2007	"Presents the process for concentrating and directly converting wave and/ or tidal energy from a water body into electrical energy".
WO2008045662	2008	"A system is adapted to extract energy from flowing liquid. It includes at least one vertically-extending vane adapted to move in response to the flowing liquid. The vane has a vertical length wherein at least a portion of the vane can be positioned below a surface of a body of liquid such that the vane forms a swept area defined at least partially by the vertical portion of vertical lengths of the vane positioned below the surface".
WO2009049269	2009	"Systems and methods for harnessing energy from ocean tides are presented, which use the rise in water level to lift a buoyant mass to an elevation and then use the weight of the mass to pressurize a working fluid, such as water, used to motivate a turbine generator to finally produce electricity".

Table 4.2. Summary of the most relevant international patents on tidal devices.

Number	Date	Description
EP1714027	2006	"A tidal power station is presented, in which a so-called submerged sail is displaced by the tide between two magazines, whereby the sail is displaced from a first magazine in the direction of a second magazine when the tide flows in a first direction, the sail being displaced in the opposite direction when the tide flows in a second direction".
EP1816345	2007	"Submersible plant for producing energy. It comprises at least one turbine and is characterized in that said turbine is mounted on a stream-driven vehicle and in that said stream-driven vehicle is secured in a structure by means of at least one wire".
EP1984572	2008	"It presents an arrangement for mounting at least one tidal turbine and its associated support structures in a river or sea bed, characterised by mounting the turbine and associated support structures upon a base/foundation structure".
EP1878913	2008	"A hydroelectric turbine for the production of electricity from tidal flow is presented. The turbine having a rotor with an open center such that the blades are mounted between an inner rim and outer rim, wherein retaining and anti-friction members are provided".
EP2013474	2009	"It shows a system for converting the kinetic energy of flowing fluid into electrical energy, through a system comprising a turbine having a low speed energy electricity generator, a shaft in communication with the generator, wherein a plurality of blades is fixable to said shaft".

Table 4.3. Summary of the most relevant European patents on tidal devices.

Type and Number	Title	Public. date	Description
US Patent Ap/ 20070284884	"Flow Enhancement For Underwater Turbine".	13/12/07	"An improved turbine generator including at least one blade and a housing disposed about said turbine, wherein the improvement comprises a slot defined by an outer and an inner surfaces, enhancing the flow characteristics".
US Patent Ap/ 20080260548	"Wave energy converter".	23/10/08	"A stationary structure is mounted on the floor of an ocean or other body of water subject to wave motion. The structure provides a floatation body that moves with the wave so is able to drive a sealing plate".
US Patent Ap/ 7470086	"Submersible tethered platform for undersea electrical power generation".	30/12/08	"A submersible platform system for carrying out repeated operations in a submarine position, and producing electrical energy".
US Patent Ap/ 20090015014	"Tidal stream energy conversion system".	15/01/09	"The present invention is concerned with an energy conversion system for converting tidal energy into electrical energy by one or more transducers forming part of the system".
US Patent Ap/ 20090015018	"Flow Stream Momentum Conversion Device Power Rotor".	15/01/09	"A device known as a FSMCD, Power Rotor is presented here. The device makes use of the principle of Conservation of Momentum to convert fluid stream input momentum to device rotational power".
US Patent/ 7479708	"Wave power converter apparatus employing independently staged capture of surge energy".	20/01/09	"A wave power converter employing independently staged surge energy capture for converting useful wave surge energy to electric power over a relatively broad range of surf conditions".
US Patent Ap/ 20090026767	"Modular system for generating electricity from moving fluid"	29/01/09	"A modular system for producing electricity from the channel, river, ocean or tidal water currents and wind is disclosed. A converter consists of a vertical axis underwater hydro-turbine connected to the electrical generator".
US Patent/ 7489046	"Water turbine system and method of operation".	10/02/09	"A system for providing electrical power from a current turbine is provided in this work. The system includes a floatation device and a set of electrical devices".
US Patent/ 7493759	"Fluid motion energy converter".	24/02/09	"A converter for producing useable energy from fluid motion of a fluid medium. The converter is supported on the support structure such that the movable element can move relatively to the structure in response to the fluid motion".

Table 4.4. Summary of the most relevant US patents on tidal devices.

The turbines used in tidal barrages are either unidirectional or bi-directional. Generating electricity using tidal barrages is mature and reliable [55]. Numerous tidal sites worldwide are considered suitable for development. Tidal barrages can be broken into two types:

- *Single-basin systems,* consist of one basin and require a barrage across a bay or estuary. There are three methods of operation: *ebb generation* (the turbine gates are kept closed until the tide has ebbed sufficiently to develop a substantial hydrostatic head across the barrage), *flood generation* (Once the sufficient hydrostatic head is achieved, the turbine gates are opened allowing the water to flow through them into the basin) and *two-way generation* (utilises both flood and ebb phases of the tide).

- *Double-basin systems*. The difference with the previous system is that a proportion of the electricity generated during the ebb phase is used to pump water into the second basin, allowing an element of storage.

Tidal current turbines extract the kinetic energy in moving water to generate electricity. Tidal current technology is similar to wind energy technology [56]. However there are several differences in the operating conditions [57]. Since tidal current turbines operate in water, they experience greater forces and moments than wind turbines. Tidal current turbines must be able to generate during both flood and ebb tides and be able to withstand the structural loads when not generating electricity. The following two methods of tidal current energy extraction are the most common [58]:

- *Horizontal axis tidal current turbines*. The turbine blades rotate about a horizontal axis which is parallel to the direction of the flow of water.

- *Vertical axis tidal current turbines*. The turbine blades rotate about a vertical axis which is perpendicular to the direction of the flow of water [59].

5 DEFINING THE CFD MODEL

5.1 Geometry and computational mesh

5.1.1 *The Porous Media Configuration*

The first results presented, describe the analyses carried out with initial turbine porous media diameters of 9 and 10m respectively, within a delta configuration. A range of angular positions of the nacelles were examined with the tidal stream flowing in the two, outgoing and incoming, tidal directions, as can be seen in Figure 5.1.

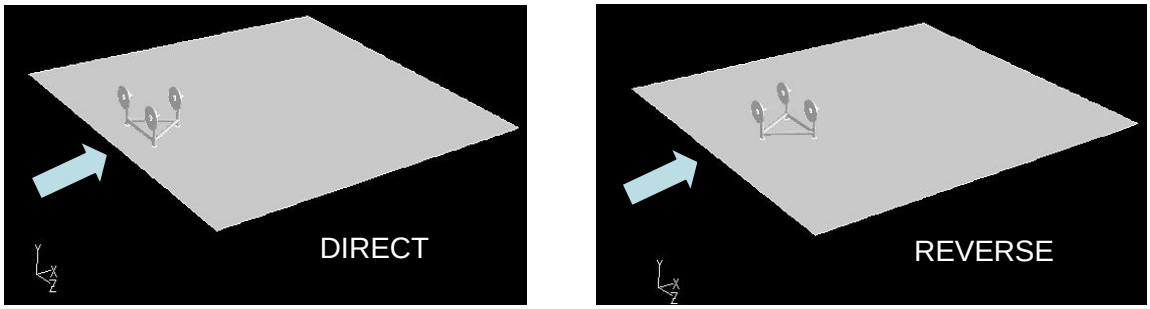

Figure 5.1. Geometry for "Direct" (left) and "Reverse" (right) configurations.

In the so called "Direct" configuration, the flow reaches first one side of the equilateral triangle with the two identical turbines on it, while the third turbine is situated right downstream. In the "Reverse" configuration, one of the vertices of the above mentioned delta is first reached with one of the turbines on it, while the two other turbines are placed right downstream.

According to this figure, the computational domain of the model was chosen to be wide enough, such is: x = 120 m., y = 40 m. and z = 108 m. while the dimensions of the Delta structure are: Equilateral triangle of L = 23 m. with the height of each column of 13.75 m. and the diameters for the porous media simulating the blades, were

considered to be 9 and 10 m respectively in order study the effect of different clearances between turbines. Other dimensions of the turbines can be seen in detail in figure 5.2.

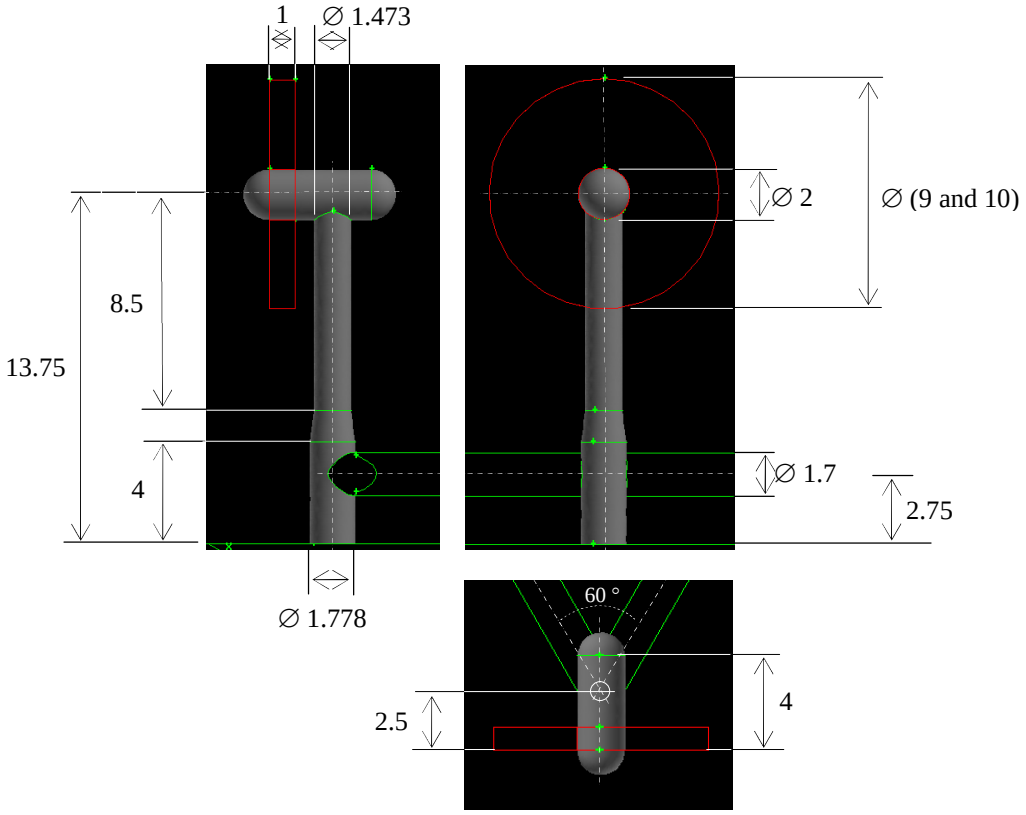

Figure 5.2. Main dimensions (m) of the turbines for the porous model.

All the boundary zones of this model are defined according to Table 5.1.

Zone	Type
Inlet	*Velocity*
Outlet	*Pressure*
Sea bed	*Wall*
Sea surface	*Symmetry*
Lateral walls	*Periodic*
Structure	*Wall*
Sea	*Fluid*
Blades	*Porous*

Table 5.1. Defining the domain of the porous model.

The grid is unstructured, containing about 2 million nodes. Figure 5.3 shows the details of the two configurations previously defined, “Direct” (a) and “Reverse” (b), both for 0 degrees (left) and 30 degrees (right) rotated discs/nacelles respectively.

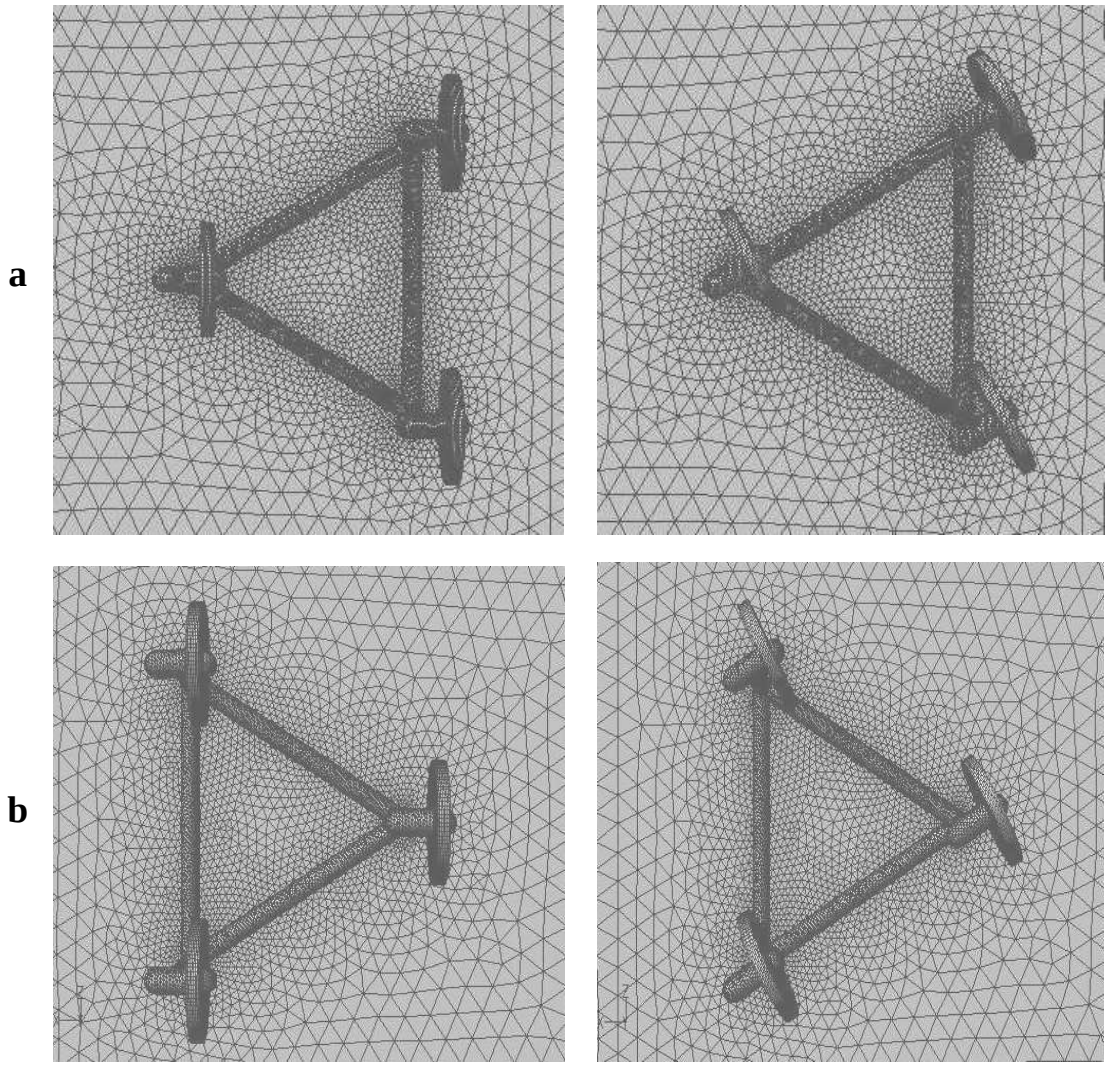

Figure 5.3. Detail of the surface grid for the DIRECT configuration (a) and REVERSE configuration (b); Both for 0 degrees (left) and 30 degrees rotated nacelles (right).

5.1.2 *The Discrete Blades Configuration*

Figure 5.4 shows a detailed view of the geometry and surface mesh corresponding to the complete structure including the three 5 m length blades. The

whole grid is unstructured, containing about 5 million nodes where nacelles can be rotated independently in a range of 0-30 degrees.

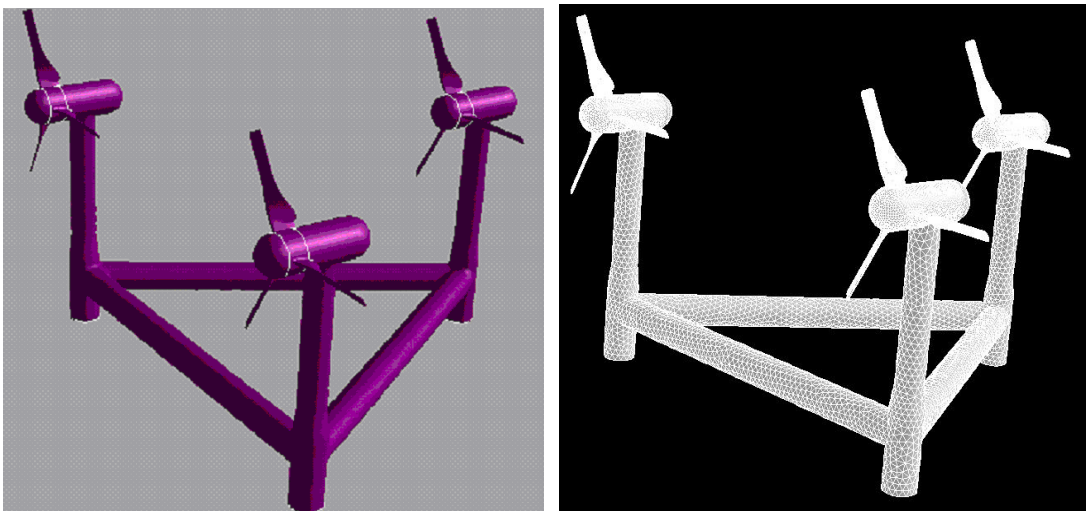

Figure 5.4. The complete tidal device geometry (left) and surface mesh (right).

The geometry of the blade was provided by the Company under a confidentiality agreement. In Figure 5.5, from left to right, the geometry of the blade used in this work can be seen, where the profiles corresponding to different sections (hub, middle and tip respectively) are depicted, showing finally the implementation in the rotor disk.

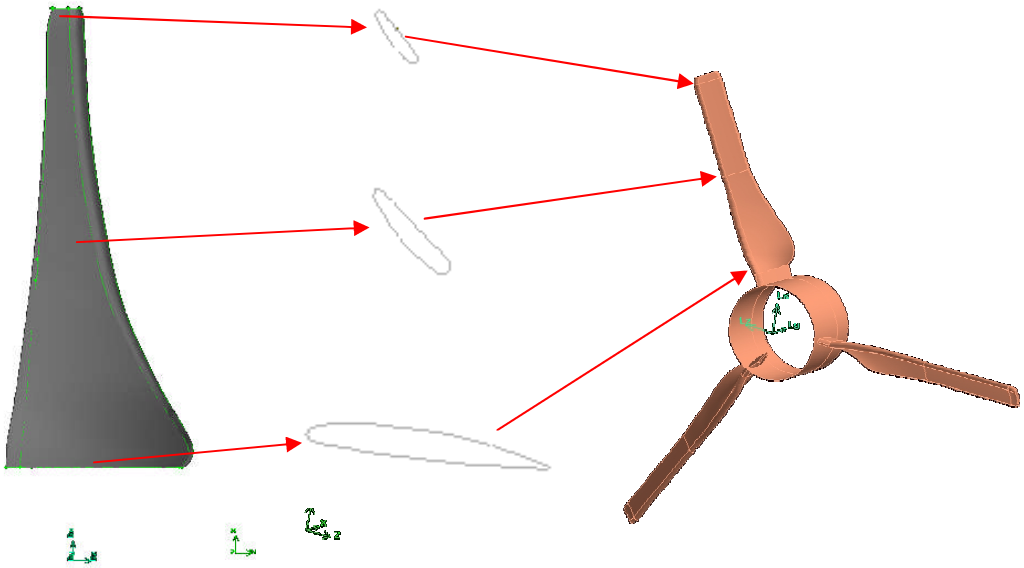

Figure 5.5. Detail of the blade geometry and further implementation in the rotor disk.

Figure 5.6 shows a detail of the mesh over a vertical plane for both frozen rotor and transient model (b), comparing to a mesh that could be used for a steady model (a). The difference between those two configurations is rather significant.

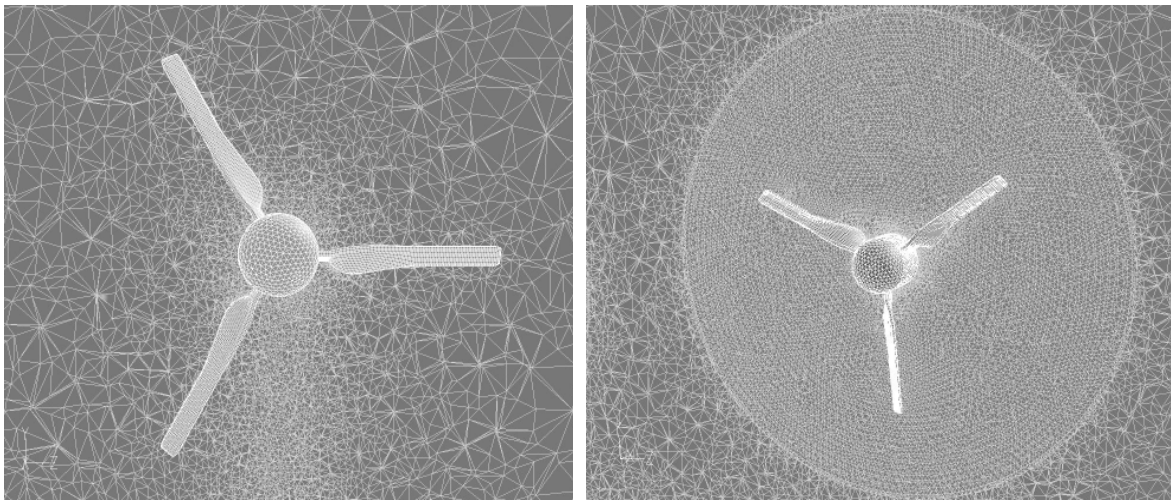

a **b**

Figure 5.6. Detail of a mesh suitable for a steady model (a) and for the unsteady models, Frozen and Transient developped in this work (b).

All the boundary zones of this model are defined through different types of cells according to Table 5.2.

Zone	Type
Inlet	*Velocity*
Outlet	*Pressure*
Sea bed	*Wall*
Sea surface	*Symmetry*
Lateral walls	*Periodic*
Structure	*Wall*
Sea	*Fluid*
Blades	*Wall*

Table 5.2. Defining the domain of the complete model.

The use of symmetry cells for the sea surface for both cases has been taken into account because the component of velocity normal to the symmetry boundary plane is set to zero which is the most apropiate condition here.

5.1.3 *Justification of the density of the grids; sensitivity analysis*

Turbulent flows are significantly affected by the presence of walls. The size of the mesh can be determined by the treatment of the turbulence in the near- wall region, in other words whether the Navier-Stokes equations need to be solved or not. For the characteristics of owr problem (high Reynolds number, low viscosity, low pressure gradient in the near- wall region) it is not necessary to solve the whole set of equations so near wall functions can be used instead, reducing the size of the mesh without affecting the accuracy of the solution.

Numerous experiments have shown that the near-wall region can be largely subdivided into three layers. In the innermost layer, called the “viscous sublayer”, the flow is almost laminar, and the (molecular) viscosity plays a dominant role in momentum and heat or mass transfer. In the outer layer, called the fully-turbulent layer, turbulence plays a major role. Finally, there is an interim region between the viscous sublayer and the fully turbulent layer where the effects of molecular viscosity and turbulence are equally important.

Anyway, the size of the adjacent near- wall cell y_p is determined depending on the choice of turbulent model used and is defined by the dimensionless term y_p^+. This parameter can be calculated according to:

$$y_p^+ \equiv y_p u_t / \upsilon \Rightarrow y_p = y_p^+ \upsilon / u_t \qquad \textbf{Equation 5.1}$$

where y_p is the distance of the centroid corresponding to the first near-wall node, per unit length, υ is the kinematic viscosity that will be defined later and u_t represents the friction velocity that can be defined as:

$$u_t \equiv \sqrt{\tau_w / \rho} = U_{mean} \sqrt{\bar{c}_f / 2}\,, \qquad \textbf{Equation 5.2}$$

where the friction coefficient is defined by:

$$\bar{c}_f / 2 \approx 0.037 (Re)^{-0.2} \qquad \textbf{Equation 5.3}$$

Next Table shows the values finally adopted:

Parameter	Value
Re	11.41 e^6
$c_f/2$	1.43 e^{-3}
u_t	0.189 m s^{-1}
υ	1.75 e^{-6} m^2 s^{-1}

Table 5.3. Main parameters for the definition of the mesh.

So finally according to equation 5.1,

$$y_p = y_p^+ \cdot 1.75 e^{-6} / 0.189 \qquad \textbf{Equation 5.4}$$

In our study, the Standard Wall Function (SWF) is used so the centroid of the adjacent cell must be in the range of: $30 \le y_p^+ \le 300$. So according equation 5.4, the distance of the centroid y_p corresponding to the first near-wall node will be in the range of: 0.277 mm y 2.77 mm. Obviously, the smaller value the higher number of cells associated (computational cost). So it is a matter of balance between accuracy and computational cost.

After several values for the first near-wall centroid were tested under this above mentioned range for the centroid, a value of 0.6mm was finally adopted, with a growing up factor of 1.2. This criterion means a final mesh size of about 2 millions nodes for the porous media model and 5 millions nodes for the transient model. Further performance of a sensitivity analysis showed irrelevant changes in the results achieved with higher number of nodes, so these values for the grid size were finally considered good enough.

5.2 Boundary conditions

The discretization used the second order upwind scheme with the exception of the pressure terms where a body-force weighted approach was implemented. The coupling of the pressure-velocity equations used the SIMPLE algorithm [60-62].

5.2.1 *The Porous Model*

The different physical aspects of flow in porous media will be described in this section. A “porous medium” or a “porous material” is a solid permeated by an interconnected network of pores filled with a fluid (liquid or gas) [25]. The study of fluid flow through porous media is increasing for the last years because the advantages of both computational time and accuracy that this simplification assumes.

There are two relevant properties defining a porous medium, such are: the porosity (ϕ) and the permeability (*K)*. On one hand, the porosity of a porous medium can be defined as [63, 64]:

$$\phi = \frac{Pore\ volume}{Matrix\ volume} \qquad \textbf{Equation 5.5}$$

Where the numerator of this equation denotes the total volume of the free space in the matrix and the denominator is the total volume of the matrix including the space occupied by the pores.

On the other hand, the permeability describes the capacity of the fluid to go through the porous medium. There are numerous relationships between these two concepts. It is of common use that *K* is found to be proportional to ϕ^m when the value of *m* depends on the geometry of the medium itself [65].

Another important topic is the "dynamic viscosity". This term indicates the resistance in the fluid due to shear but also angular deformations [32]. Another expression for the viscosity is the "kinematic viscosity" (υ), defined as:

$$\upsilon = \mu / \rho \qquad \textbf{Equation 5.6}$$

Where μ and ρ are respectively the dynamic viscosity and the density of the fluid (sea water). The viscosity of incompressible Newtonian fluids such as water can be assumed to be isotropic, so they are characterized by a constant viscosity coefficient. Then the flow rate of the fluid trough this medium is given by Darcy's equation [62, 67] for the main flow direction:

$$U = -\frac{K}{\mu} \cdot \left(\Delta P - \rho g \right) \qquad \textbf{Equation 5.7}$$

Where, U represnts the mean velocity of the fluid while *g* is the acceleration due to gravitational forces.

In essence, the porous media model is nothing more than an added momentum sink in the governing momentum equations. As such, the following modelling limitations should be readily recognized:

- The fluid does not accelerate as it moves through the medium, since the volume blockage which is present physically is not represented in the model. This may have a significant impact in transient flows since

it implies that the transit time for flow through the medium is not correctly represented.

- The effect of the porous medium on the turbulence field is only approximated.

The theoretical pressure drop per unit length was predicted using the following relation [62, 67]:

$$\Delta p = \frac{1}{K} \cdot \mu \cdot U_{mean} + \frac{1}{2} C_2 \cdot \rho \cdot U_{mean}^2 \qquad \textbf{Equation 5.8}$$

where the values finally adopted for the most important coefficients in this study, can be seen summarised next in Table 5.4.

Item	Name	Value
Δp	Pressure drop per unit length	2,000 Pa m^{-1}
$1/K$	Viscous resistance	1 10^{10} m^{-2}
μ	Water viscosity at 25 ºC	1.08 10^{-3} Pa s
ρ	Seawater density at 25 ºC	1,025 kg m^{-3}
C_2	Inertial resistance factor	100 m^{-1}

Table 5.4. Values adopted for the porous media model.

When dealing with a simple homogeneous porous media, the source term is composed of two parts, a viscous loss term (Darcy), and an inertial loss term as can be seen in the next equation [68] for the case of a sinple homogeneous porous media.

$$S_i = \frac{\mu}{\alpha} \cdot v_i + C_2 \cdot \frac{1}{2} \cdot \rho \cdot |v_i| \cdot v_i \qquad \textbf{Equation 5.9}$$

where, S_i is the source term and v_i the velocity for the i th (x, y, or z) momentum equation. This momentum sink contributes to the pressure gradient in the porous cell, creating a pressure drop that is proportional to the fluid velocity (or velocity squared) in the cell [69].

FLUENT® will, by default, solve the standard conservation equations for turbulence quantities in the porous medium. In this default approach, therefore, turbulence in the medium is treated as though the solid medium has no effect on the turbulence generation or dissipation rates [69]. Turbulent flows are characterized by fluctuating velocity fields. These fluctuations mix transported quantities such as momentum, energy, and species concentration, and cause the transported quantities to fluctuate as well. Since these fluctuations can be of small scale and high frequency, they are too computationally expensive to simulate directly in practical engineering calculations. Instead, the instantaneous (exact) governing equations can be time-averaged, ensemble-averaged, or otherwise manipulated to remove the resolution of small scales, resulting in a modified set of equations that are computationally less expensive to solve. However, the modified equations contain additional unknown variables, so turbulence models are needed to determine these variables in terms of known quantities.

When using one of the k-ε turbulence models or the Spalart-Almaras model, the effect of turbulence in a porous region can be suppressed by setting the turbulent contribution to viscosity, μ_t, equal to zero [62]. Then the inlet turbulence quantities will be transported through the medium, but their effect on the fluid mixing and momentum will be ignored. The selection of a turbulence model depends on considerations such as the physics of the flow, the well-known experience for a specific case, the accuracy required, the available computational resources, and of course the time available for the simulation. Next an introduction to the turbulence models chosen for this work is given.

5.2.2 *The k-ε Model (REALIZABLE)*

The governing Reynolds-averaged equations for continuity and momentum conservation were used. The Realizable k-ε model was used to close the governing

equations, which is a semi-empirical model based on the model transport equations for the turbulent kinetic energy (*k*) and dissipation rate (*ε*). The model transport equation for *k* is derived from the exact equation, while the transport equation for *ε* is obtained using physical reasoning and bears little resemblance to its mathematically exact counterpart.

In the derivation of the *k*-*ε* model, it was assumed that the flow is fully turbulent. The realizable *k*-*ε* models provide better results than the standard k-*ε* model, thanks to their modifications for adverse pressure gradient flows.

The word “Realizable” actually implies that the model satisfies specific constraints on the Reynold's stresses that make the model more consistent with the physics of turbulent flows and hence more accurate than the standard k- *ε* model.

This model makes the eddy-viscosity coefficient, C_v, dependent on the mean flow and turbulence parameters. The notion of variable C_v has been suggested by many authors and is well substantiated by experimental evidence [62, 64]. For example, Cv is found to be around 0.09 in the defect layer of an equilibrium boundary layer, but only 0.05 in a strong shear flow. Note that in the realizable model, Cv can be shown to recover this standard value of 0.09 for simple equilibrium flows [65-68]. Transport equations for *k* and *ε* respectively are as follows:

$$\frac{D}{Dt}(\rho\, k) = \frac{\partial}{\partial x_j}\left[\left(\mu + \frac{\mu_t}{\sigma_k}\right)\frac{\partial\, k}{\partial x_j}\right] + G_k - \rho\, \varepsilon \qquad \textbf{Equation 5.10}$$

$$\frac{D}{Dt}(\rho\, \varepsilon) = \frac{\partial}{\partial x_j}\left[\left(\mu + \frac{\mu_t}{\sigma_\varepsilon}\right)\frac{\partial\, \varepsilon}{\partial x_j}\right] + C_{g1}\cdot\frac{\varepsilon}{k}\cdot G_k - \rho\cdot C_{g2}\cdot\frac{\varepsilon^2}{k} \qquad \textbf{Equation 5.11}$$

And the constants used in the present work for this model [69] can be seen in Table 5.5:

Item	Value
σ_k	1
c_υ	0.09
σ_t	1.3
C_{g1}	1.44
C_{g2}	1.92

Table 5.5. Constants of the transport equations for the k-ε (REALIZABLE).

5.2.3 *The SST k-ω Model*

The turbulence model finally chosen for the unsteady models was the SST k-ω. The use of a k-ω formulation in the inner parts of the boundary layer makes the model directly usable all the way down to the wall through the viscous sub-layer, hence the SST k-ω model can be used as a Low-Re turbulence model without any extra damping functions [70-72]. The SST formulation avoids the common k-ω problem that the model is too sensitive to the inlet free-stream turbulence properties. It is characterised for its good behaviour in adverse pressure gradients and separating flow.

This model does produce a bit too large turbulence levels in regions with large normal strain, like stagnation regions and regions with strong acceleration. This tendency is much less pronounced than with a normal k-ε model [73-76]. Transport equations for *k* and ω respectively are as follows:

$$\frac{\partial k}{\partial t}+U_j\frac{\partial k}{\partial x_j}=P_k-\beta^* k\omega+\frac{\partial}{\partial x_j}\left[\left(\nu+\sigma_k\nu_t\right)\frac{\partial k}{\partial x_j}\right] \qquad \textbf{Equation 5.12}$$

$$\frac{\partial \omega}{\partial t}+U_j\frac{\partial \omega}{\partial x_j}=\alpha S^2-\beta\omega^2+\frac{\partial}{\partial x_j}\left[\left(\nu+\sigma_\omega\nu_t\right)\frac{\partial \omega}{\partial x_j}\right]+2\left(1-F_1\right)\sigma_\omega\frac{1}{\omega}\frac{\partial k}{\partial x_i}\frac{\partial \omega}{\partial x_i} \qquad \textbf{Equation 5.13}$$

And the constants used in the present work for this model [69] can be seen in Table 5.6:

Item	Value
σ_k	0.85
σ_ω	0.856
β^*	9/100
α	0.44

Table 5.6. Constants of the transport equations for the *SST* k-ω turbulence model

6 RESULTS AND DISCUSSION

To gain an understanding of how different factors impact on the far wake flow field, data has been visualised on both, velocity fields and total pressure plots.

6.1 The porous model

On one hand, two cases have been studied regarding the diameter of the rotor disc such as 9 and 10 meters respectively (in both configurations direct and reverse), in order to compare the effects that the size of the rotors has on the flow interference. On the other hand a range of rotational degrees from 0º to 30º for the nacelle's yaw has been also taken into account in order to compare the effects that the relative rotation angle of the rotors has also on the flow interference.

Figure 6.1 shows the velocity field over a symmetry vertical plane for the direct configuration (left) and reverse configuration (right) for a 0 degrees rotation of the nacelles. The effect over the downstream turbine is not negligible.

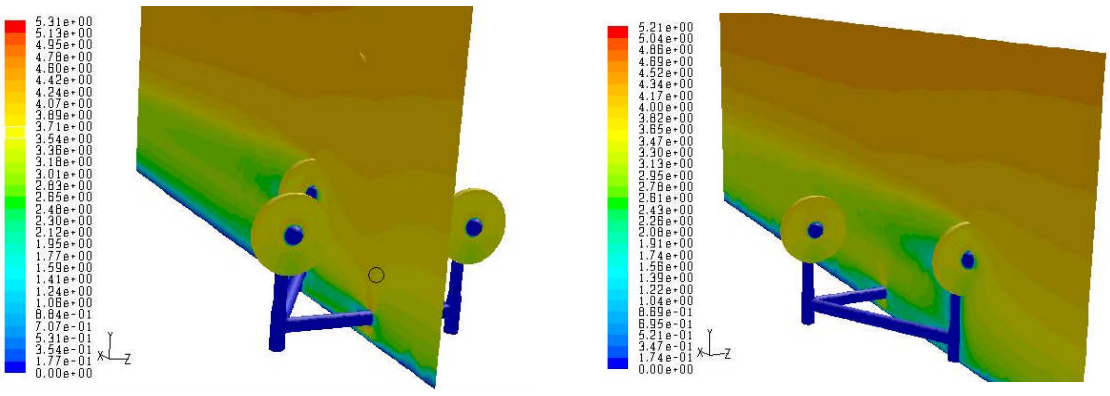

Figure 6.1. Comparative velocity field over a vertical symmetry plane (0 degrees).

6.1.1 *The 9 m. diameter rotor disc*

Figures 6.2 and 6.3 show a comparative velocity / total pressure field for different rotation degrees (0, 15 and 30 degrees respectively) for both the DIRECT and REVERSE configurations respectively, corresponding to the 9 m. diameter rotor disc.

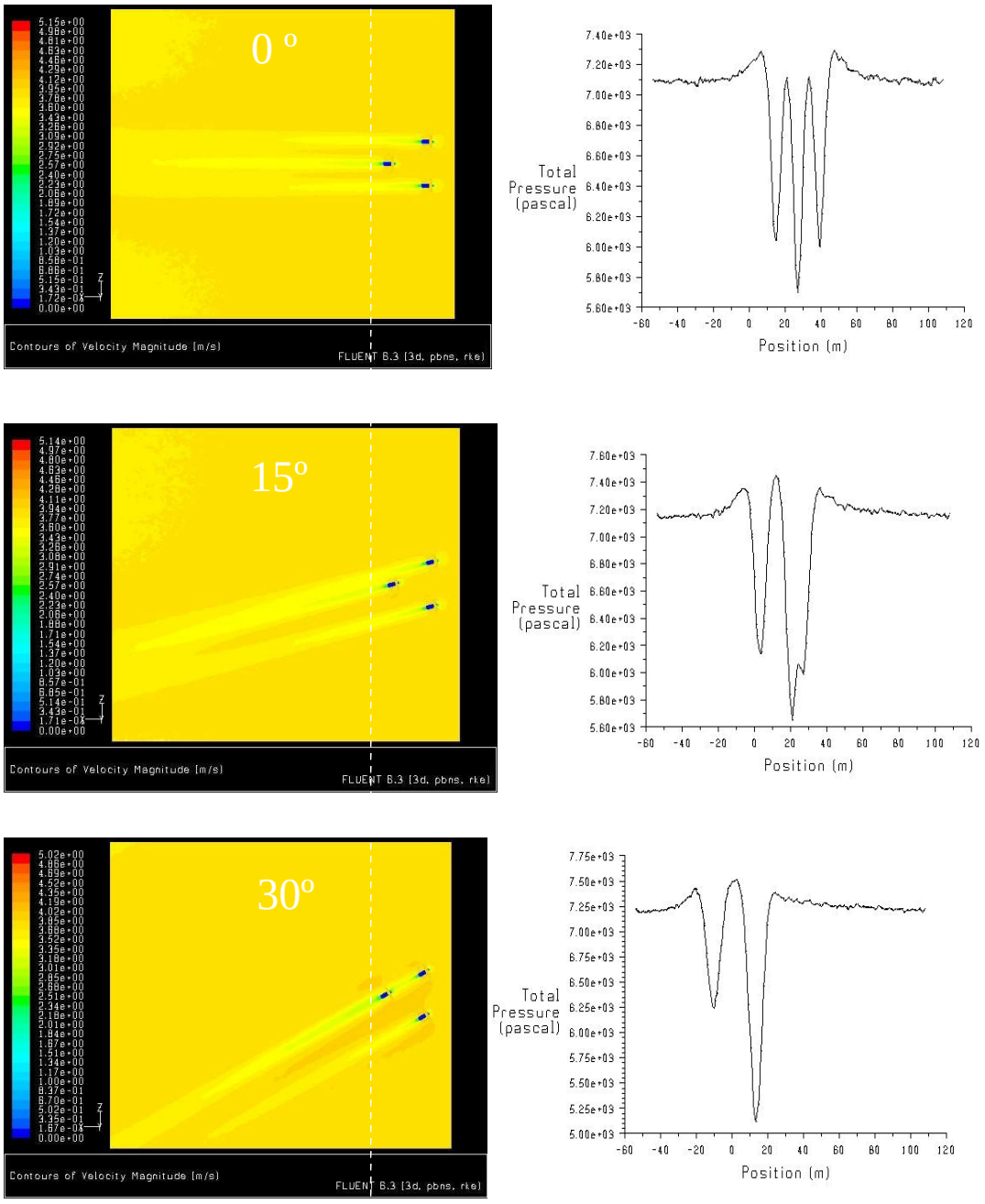

Figure 6.2. Velocity field over a plane of y = 13.75 m for different rotation degrees (left) and the corresponding total pressure plots over a plane of x = 30 m (right) for the DIRECT 9 m configuration

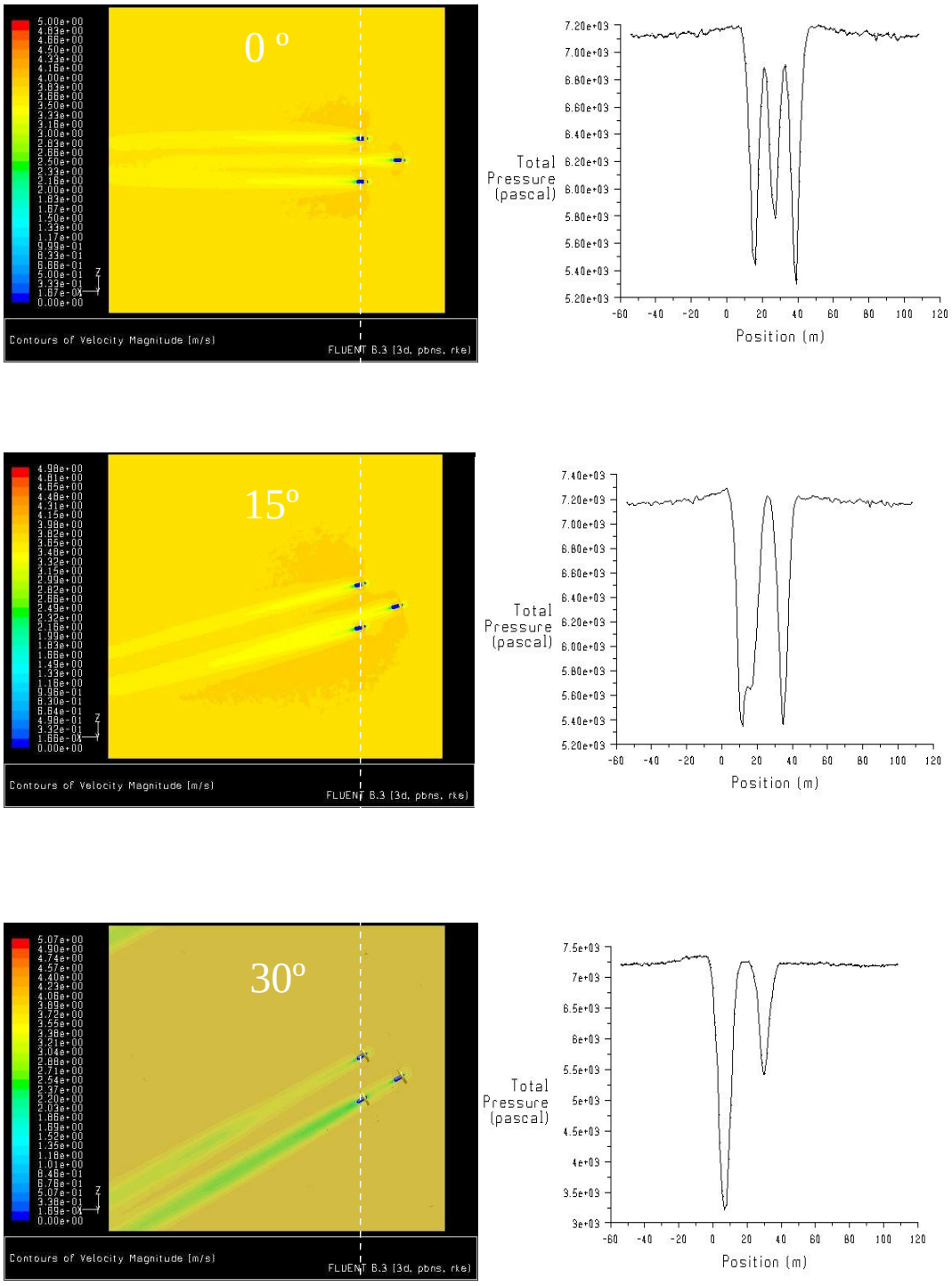

Figure 6.3. Velocity field over a plane of y = 13.75 m for different rotation degrees (left) and the corresponding total pressure plots over a plane of x = 30 m (right) for the REVERSE 9 m configuration.

6.1.2 *The 10 m. diameter rotor disc*

Figures 6.4 and 6.5 show a comparative velocity / total pressure field for different rotation degrees (0, 15 and 30 degrees respectively) for both the DIRECT and REVERSE configurations respectively, corresponding to the 10 m. diameter rotor disc.

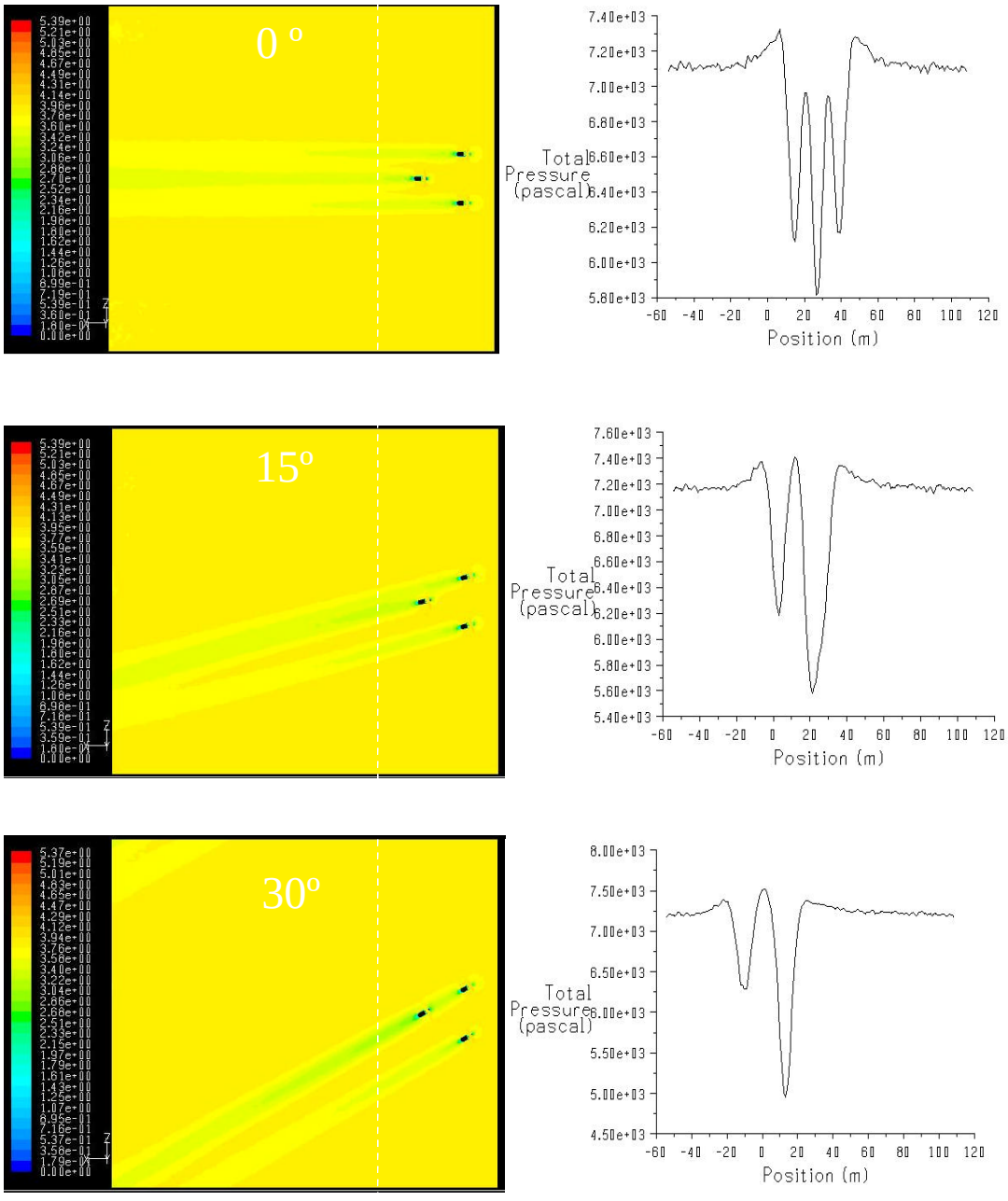

Figure 6.4. Velocity field over a plane of y = 13.75 m for different rotation degrees (left) and the corresponding total pressure plots over a plane of x = 30 m (right) for the DIRECT 10 m configuration.

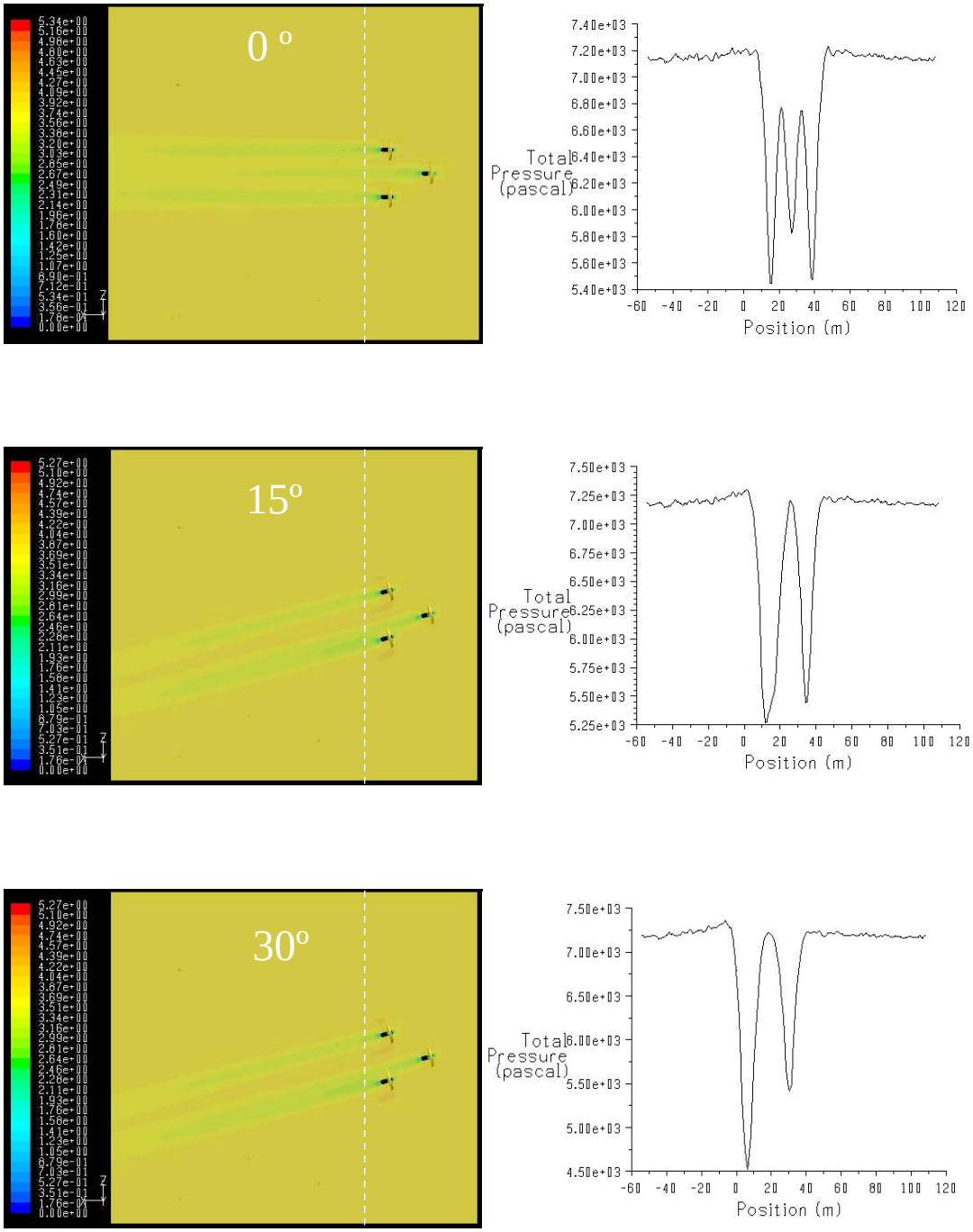

Figure 6.5. Velocity field over a plane of y = 13.75 m for different rotation degrees (left) and the corresponding total pressure plots over a plane of x = 30 m (right) for the REVERSE 10 m configuration.

6.1.3 *Discussion of the results*

Figures 6.2 to 6.5 show the degree of interference that may occur between the turbines of this marine device as the nacelles are yawed onto a range of angular settings (0-30 degrees) with the tidal stream flowing in the two, outgoing and incoming directions. Only intermediate positions (0-15 and 30 degrees) have been shown. Total pressure plots of the wake present an unusual increasing of the total pressure in the area surrounding the wakes. This is probably due to a combination of the turbulent shear layer and the bounding free surface forcing a greater proportion of flow over the disc.

Where turbines are in line with each other, then the development of the flow downstream from a turbine is of interest. This information will be used for the optimum positioning of the other turbines. Figure 6.6 shows the velocity magnitude of the fluid along the turbine axis upstream and downstream the turbine, as a percentage of the free stream velocity (%). The turbine is positioned as a reference at the 0 datum. As can be seen in this figure, upstream the turbine, as the fluid approaches the turbine from left to right, the velocity drops. Immediately behind the hub of the turbine a large recirculation zone can be observed, which forces the velocity magnitude to a substantial increase. Downstream the turbine the fluid gradually tries to recover [20].

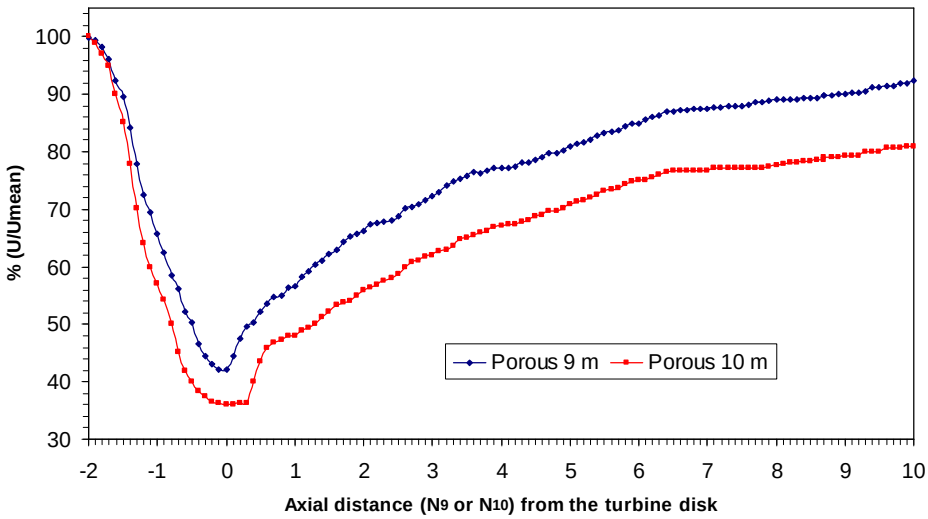

Figure 6.6. Development of the flow downstream the turbine for the 9 and 10 m configurations.

According to this figure, the fluid reaches 80% of the free stream velocity at approximately 4.8 turbine diameters downstream of the 9 m rotor disc turbine configuration (approximately 43 m.) and approximately 9.2 turbine diameters downstream of the 10 m rotor disc turbine (approximately 92 m.). A 90% recovery is achieved however after the 80 m. downstream of the 9 m rotor disc turbine configuration, being out of range for the 10 m rotor disc configuration.

From the same figure, can be deduced that when the turbines are of alignment in the Delta structure (23 m length), only a 69 % velocity recovery would be achieved according to the 9 m rotor disc turbine (blue dashed line) whereas only a 58 % velocity recovery would be achieved for the 10 m rotor disc turbine (red dashed line). This allows us to estimate the decreasing of the efficiency of the turbine directly affected in the same amount.

Figure 6.7 shows the increase of the area ratio with the yaw angle of the nacelle, for a range from 0-30 degrees for both configurations, such as 9 m and 10 m respectively. This ratio can be defined as the rotor disc area directly affected for the wake of an upstream turbine placed at a distance of 23 m (delta configuration) divided by the total rotor disc area. As can be seen in this figure, the area directly affected by the upstream wake shows a fast increase for the 10 m configuration with respect to the increase for the 9 m configuration. For both profiles the 100 % of the area directly affected is reached for a yaw angle of 30 degrees.

Figure 6.8 shows the percentage of decrease of the pressure ratio, as a function of the yaw angle in a range from 0-30 degrees for both configurations, such as 9 m and 10 m respectively. This ratio can be defined as the pressure due to the wake of an upstream turbine (corresponding to the delta configuration) divided by the mean operating pressure.

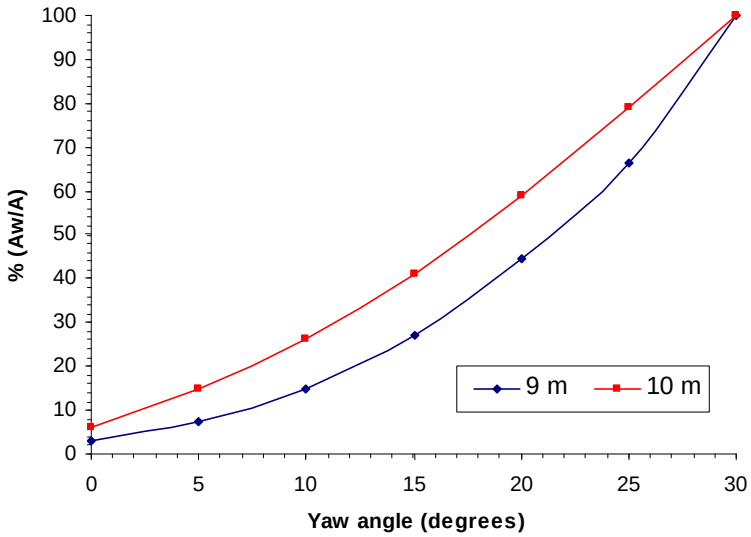

Figure 6.7. Area ratio (%) as a function of the yaw angle (degrees) for both configurations.

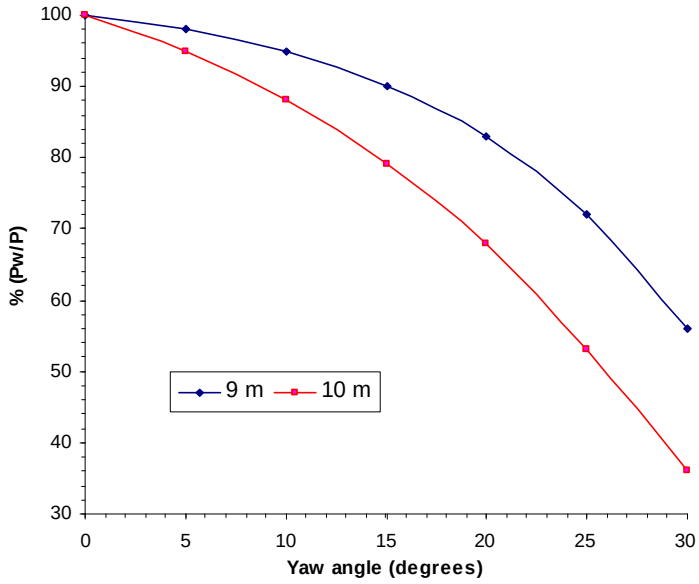

Figure 6.8. Pressure ratio (%) as a function of the yaw angle (degrees) for both configurations.

6.2 The discrete blades model

The following results obtained with models which contain discrete blade representations will be shown. These models comprise the “frozen rotor” and the “transient”.

6.2.1 *The frozen rotor*

In figure 6.9, absolute velocity vectors for the DIRECT configuration are depicted in a horizontal plane so the main recirculation area for each turbine is just shown downstream each blade although another recirculation zone is obviously registered right behind each nacelle.

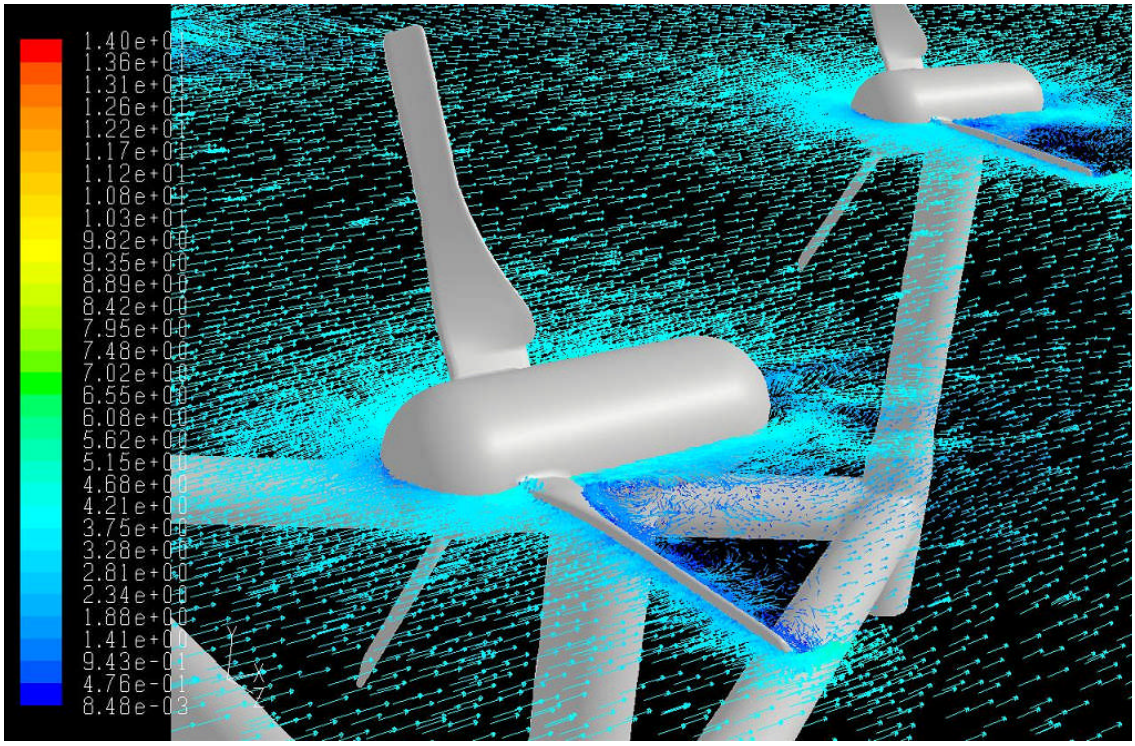

Figure 6.9. Vectors of velocity over a horizontal plane for 0 rotation degrees (frozen rotor).

Figure 6.10 shows a comparative test of velocity contours in a horizontal plane corresponding to the nacelles height and its respective total pressure plots in the plane of about 30 m downstream the inlet (white dashed line) for different rotation degrees (0,

15 and 30 degrees respectively) for the DIRECT configuration, corresponding to the frozen rotor model.

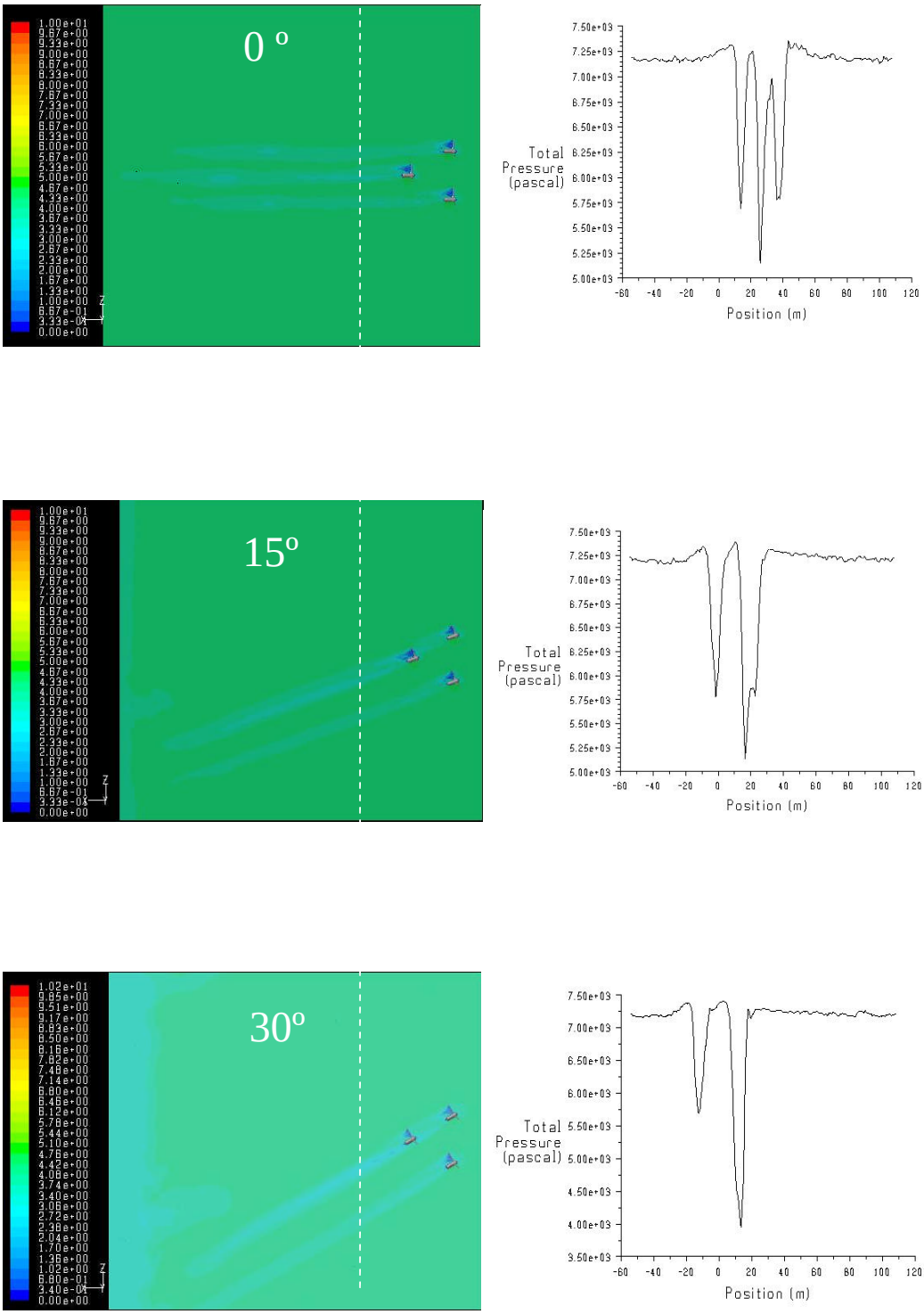

Figure 6.10. Velocity field over a plane of y = 13.75 m for different rotation degrees (left) and the corresponding total pressure plots over a plane of x = 30 m (right) for the frozen rotor, DIRECT configuration.

These velocity contours show acceptable agreement with the ones shown in figures 6.2 and 6.4 respectively, corresponding to the DIRECT configuration for both, 9 and 10 m rotor disc porous models.

6.2.2 *The transient model*

Figure 6.11 shows a velocity field over a vertical front plane, situated immediately downstream of the plane of turbine blades, so the rotational effect induced to the flow can be clearly assesed here as blades have been imposed a rotational speed of 15 rpm, according to available data [20]. The timestep is: $5e^{-3}$ s and the total time considered was 30 s.

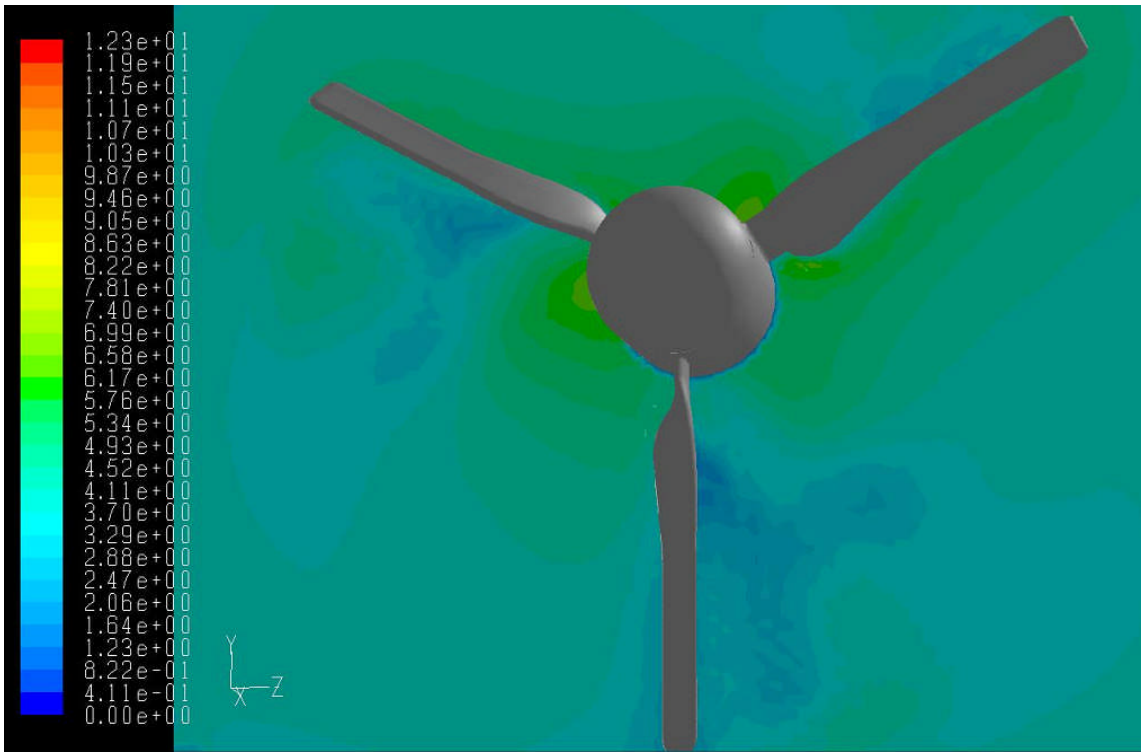

Figure 6.11. Velocity field over a front plane for 0 rotation degrees (transient model).

Figure 6.12 shows the wake caused on the flow according to the transient model for the DIRECT configuration for various degrees of rotation of the nacelles and the respective total pressure plots in the same plane of reference (white dashed line). From

these figures the discrepancy can be directly observed, in terms of wake shape, when comparing with the results offered in figure 6.10 corresponding to the "frozen rotor" scheme.

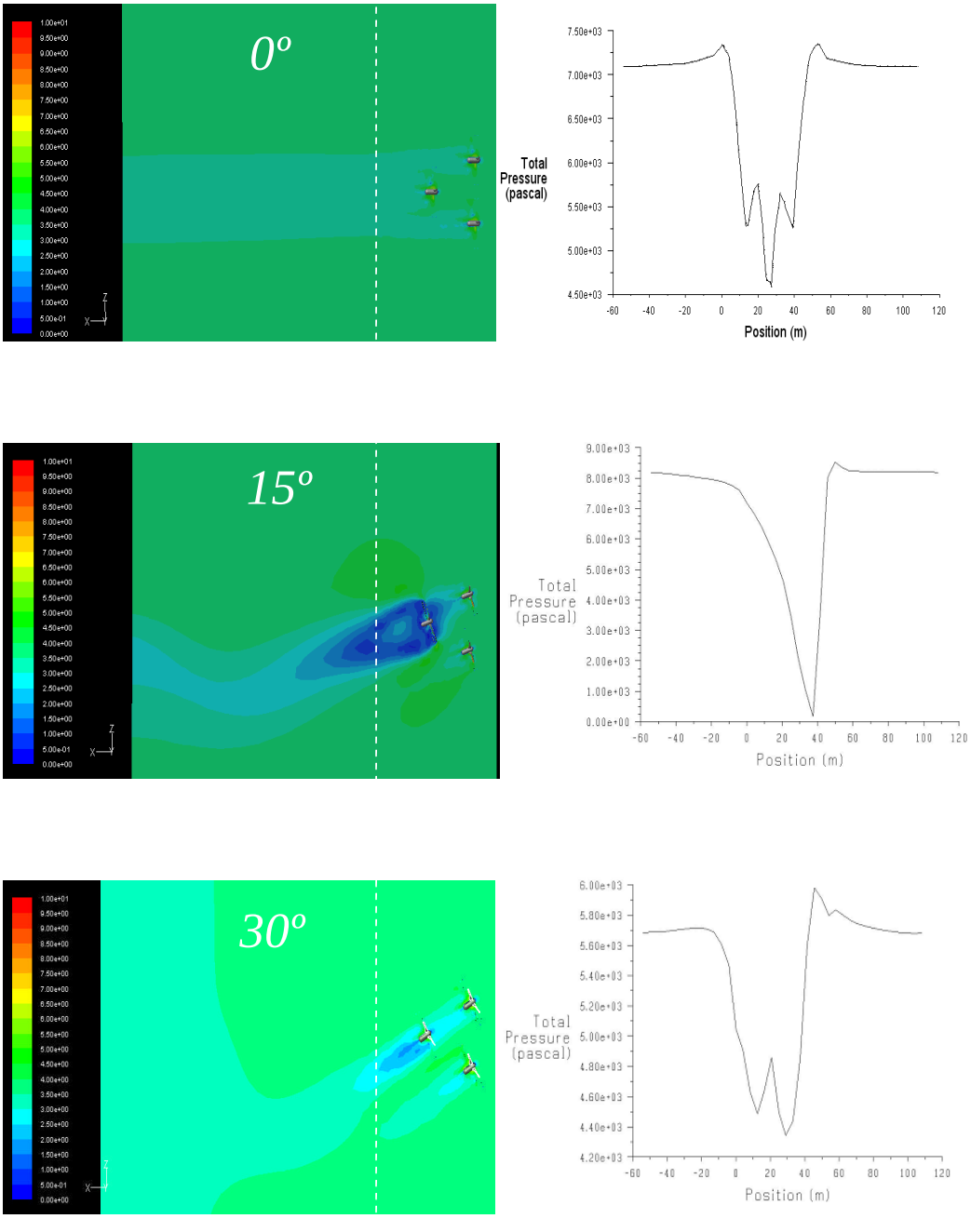

Figure 6.12. Velocity field over a plane of y = 13.75 m for three rotation settings (left) and the corresponding total pressure plots over a plane of X = 30 m (right) for the transient, DIRECT configuration.

Figure 6.13 shows the wake caused on the flow according to the "rotating blades" model for the REVERSE configuration, in this case only the 0 degrees of rotation for the nacelles and the respective total pressure plot in the plane of reference (white dashed line) has been depicted as the paterns for the other degrees are rather repetitive.

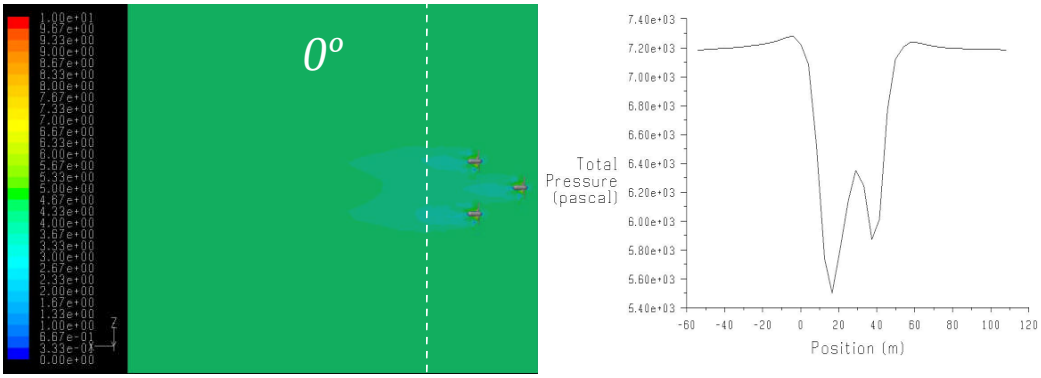

Figure 6.13. Velocity field over a plane of y = 13.75 m for different rotation degrees (left) and the corresponding total pressure plots over a plane of X = 30 m (right) for the transient, REVERSE configuration.

The most relevant differences reached with this configuration of rotating blades when compared with the frozen rotor scheme, must be pointed out. First of all there are slightly differences in the shape of the wake as have been previously commented. Thus, when comparing figure 6.10 (frozen rotor simulations) and figure 6.12 (transient simulations), both of them for the DIRECT configuration, a longer wake has been identified with the first one. Apart from this, the pressure plots are also rather different not in average values but in the shape itself, showing a more smoothed shape with the last model, indicating that a more gradual variation of the total pressure along this plane of reference occurs.

Figure 6.14 shows this variation in velocity in a vertical plane (symmetry plane) for two different positions of the nacelles (0 and 30 yaw degrees respectively) for the DIRECT configuration. The effect over the downstream turbine is more than evident,

especially when the nacelles are rotated according to the above mentioned figure, showing the maximum interaction for a yaw angle of 30 degrees for the nacelles.

a

b

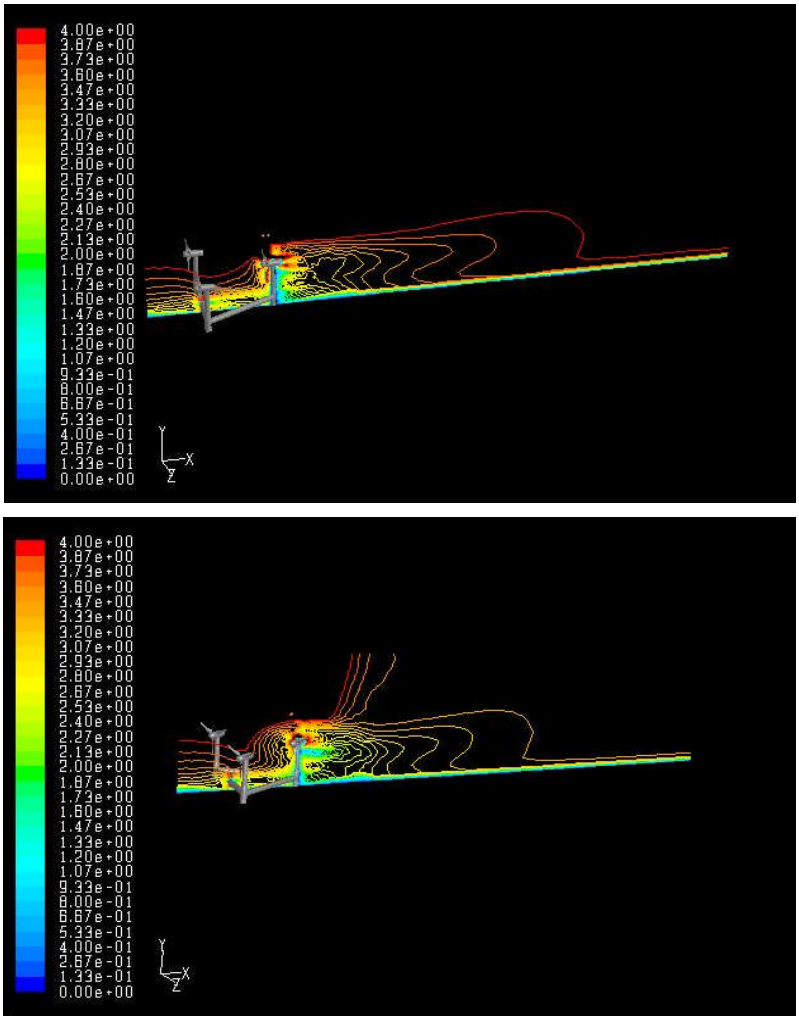

Figure 6.14. Comparative effect of the yaw angle over the flow in a symmetry plane for 0 degrees (a) and 30 degrees (b) for the transient, DIRECT configuration.

Figure 6.15, shows the effect of both flow velocity and yaw angle of the nacelles on the wakes created through the delta arrangement for the rotating blades configuration (DIRECT). All the pictures show surfaces of constant velocity in a range between 3.0 and 3.6 m/s while for the rotation of the nacelles only the extreme values such as 0 and 30 degrees are depicted in order to visualize in deep the wakes, especially on the downstream turbine. When considering high values for both velocity and yaw angles, the downstream flow is seriously affected.

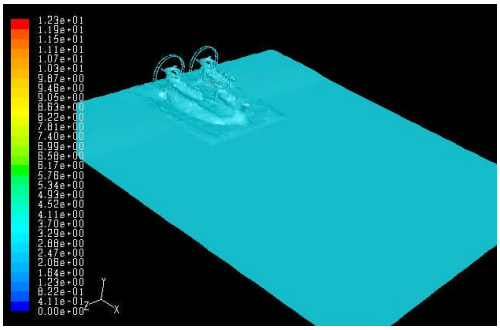

3.0 m/s 0 degrees

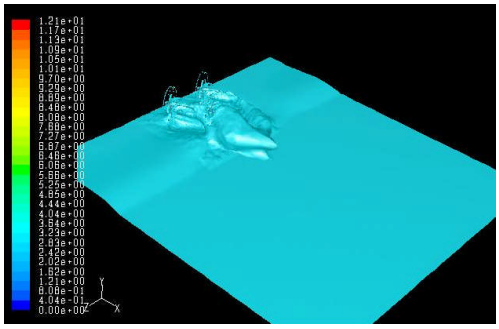

3.0 m/s 30 degrees

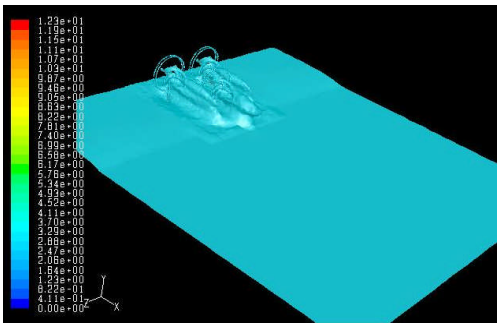

3.2 m/s 0 degrees

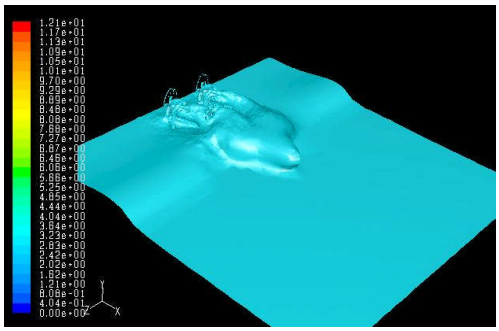

3.2 m/s 30 degrees

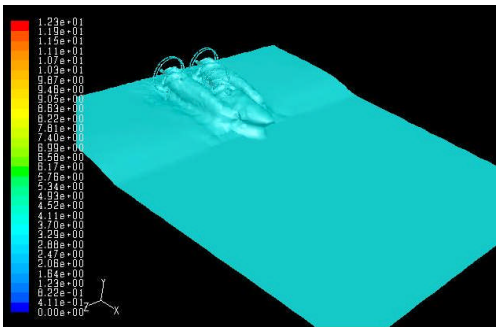

3.4 m/s 0 degrees

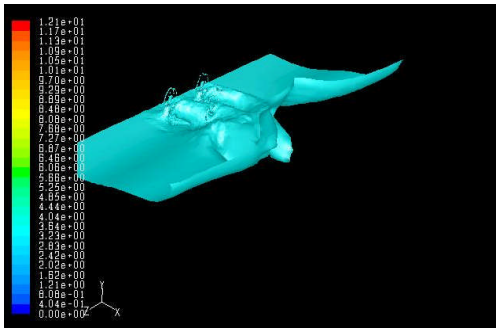

3.4 m/s 30 degrees

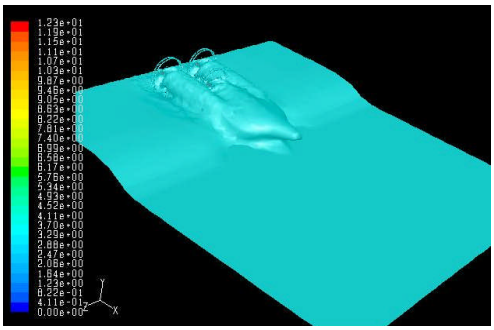

3.6 m/s 0 degrees

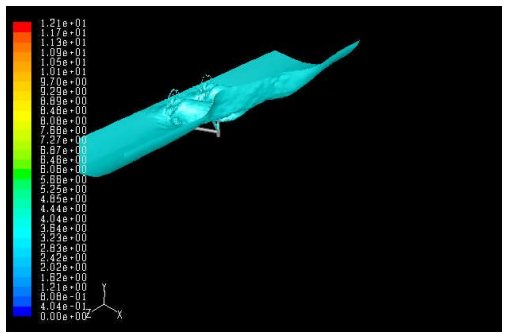

3.6 m/s 30 degrees

Figure 6.15. Combined effect of velocity and yaw angle over the flow for the transient, DIRECT configuration.

Figure 6.16 shows the variation in velocity in the vertical plane of symmetry (up) and in a horizontal plane (down) for 0 degrees angles of the nacelles for the REVERSE configuration. The effect over the downstream turbines is not as evident as it was with the DIRECT configuration.

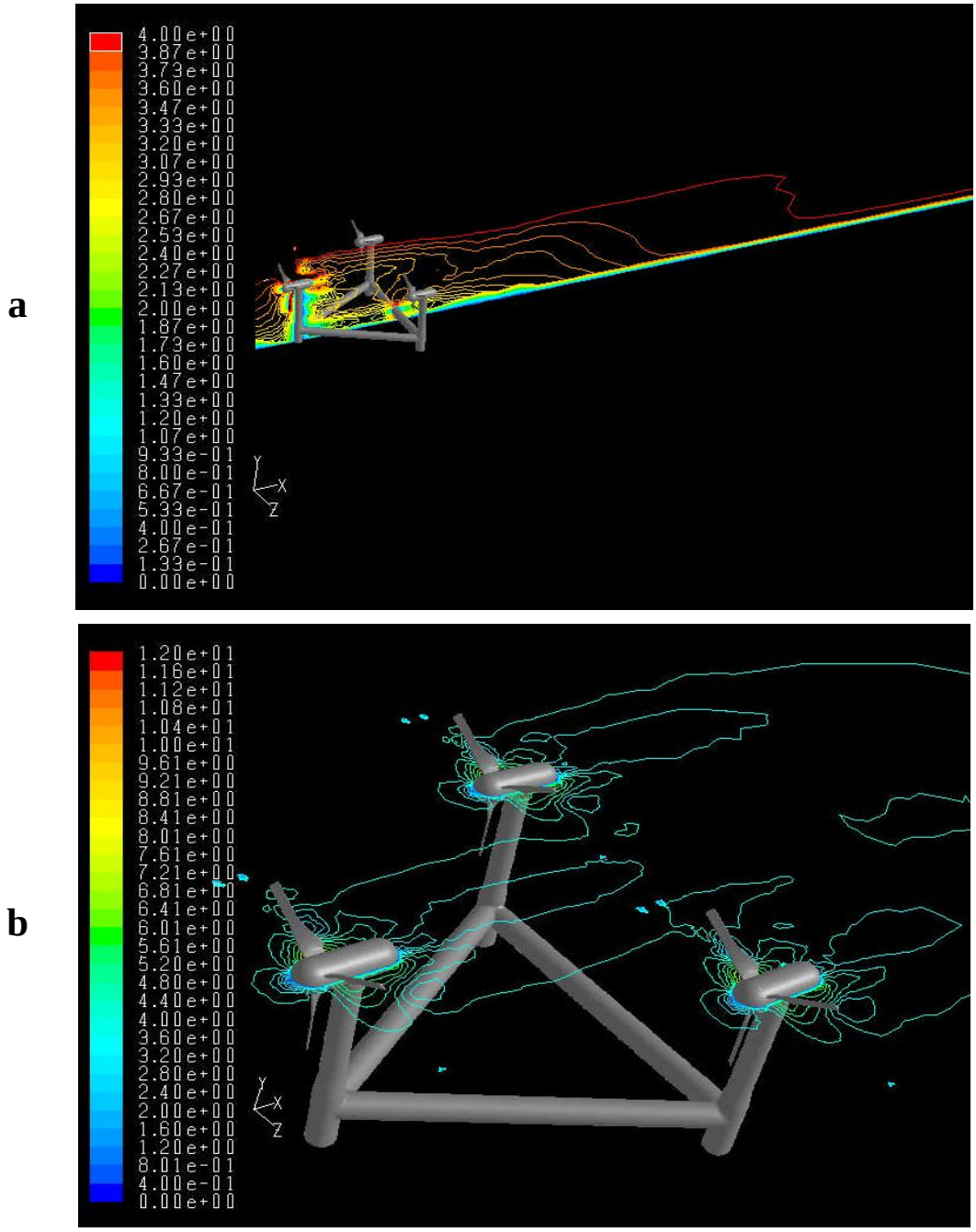

Figure 6.16. Turbine interactions in a symmetry plane (a) and in a horizontal plane (b) for the transient, REVERSE configuration.

Figure 6.17, shows the effect of both the velocity on the wakes created through the delta arrangement for the rotating blades configuration (REVERSE). All the pictures show surfaces of constant velocity in a range between 3.0 and 3.6 m/s in order to visualize in deep the wakes, especially on the downstream turbines.

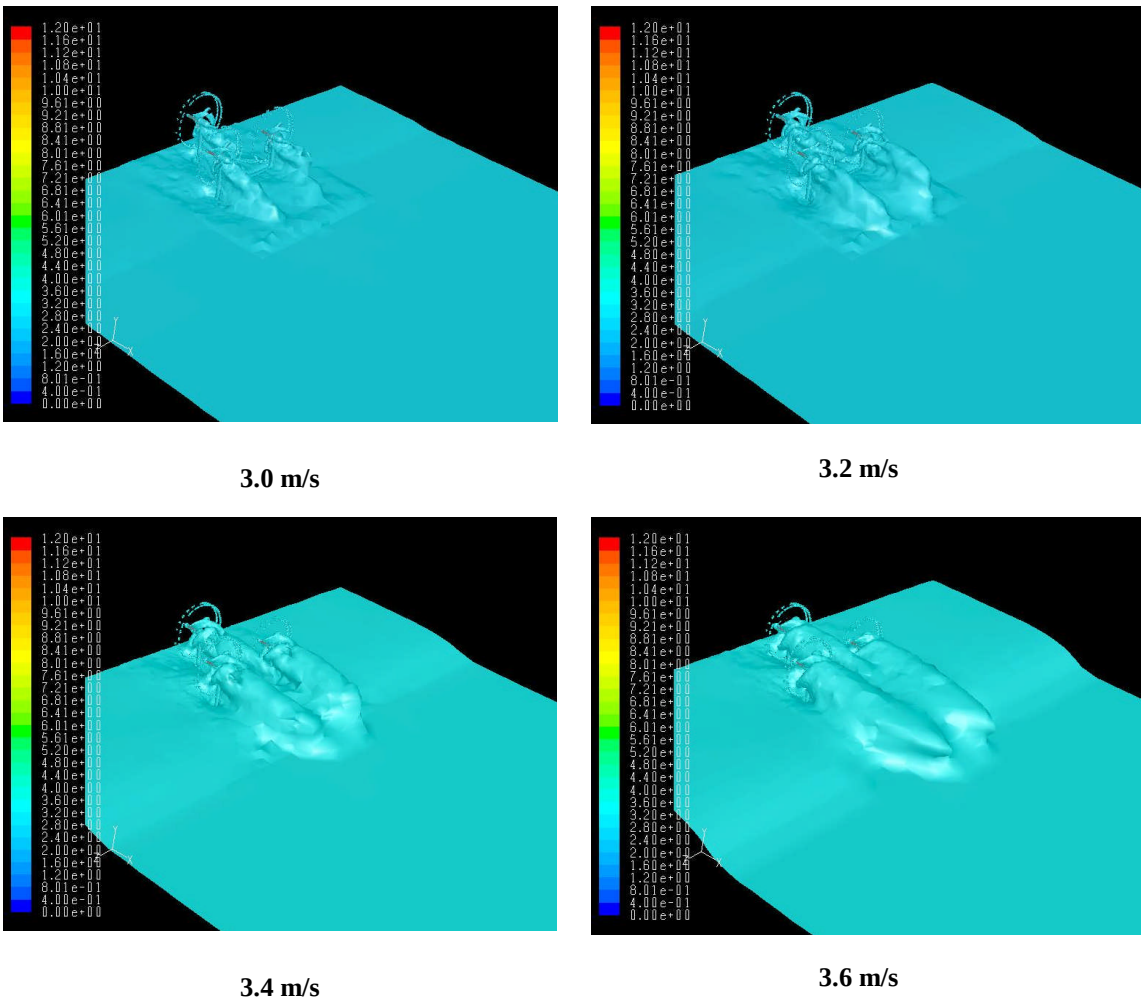

3.0 m/s **3.2 m/s**

3.4 m/s **3.6 m/s**

Figure 6.17. Effect of velocity over the flow for the 0 degrees transient, REVERSE configuration.

6.2.3 *Discussion of the results*

With reference to the partially unsteady model, “Frozen rotor”, but also to the fully unsteady “transient model”, *SST-kω* turbulence model has been considered as the best approach. A huge computational effort was needed for the last model, and a severe

grid refinement was performed manually in specific areas of the interaction between fluid and blades, more precisely in areas closer to the tip of the blades, as was previously shown in figure 5.5 (b).

Figures 6.10 and 6.12 showed the degree of interference that may occur between the turbines of this marine device as the nacelles are yawed onto a range of angular settings (0-30 degrees) with the tidal stream flowing in the two, outgoing and incoming directions. Only intermediate positions (0-15 and 30 degrees respectively) were shown. Pressure plots of the wake also present an unusual increase of the total pressure in the area surrounding the wakes. This is probably due to a combination of the turbulent shear layer and the bounding free surface that forces a greater proportion of flow over the blades.

Where turbines are in line with each other, as can be seen in figure 6.18, the development of the flow downstream of a turbine is of a real concern as this information would lead for the optimum settlement of the downstream turbines.

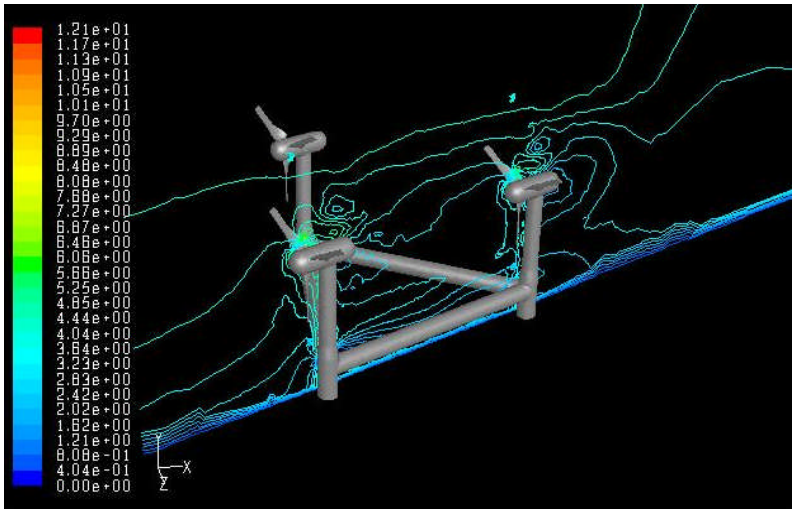

Figure 6.18. Development of the flow when two turbines are aligned.

Figure 6.19 shows the velocity magnitude of the fluid along the turbine axis upstream and downstream the turbine, as a percentage of the free stream velocity (%). The turbine is positioned as a reference at 0 m. Upstream of the turbine, as the fluid

approaches the turbine from left to right, there is a significant velocity drop. Downstream the turbine the fluid gradually would recover the original value [20].

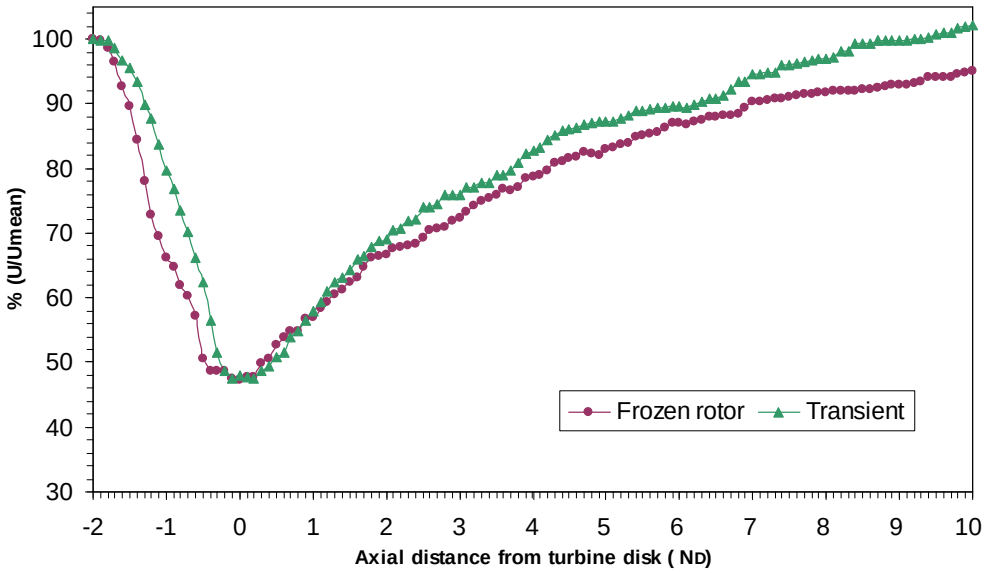

Figure 6.19. Development of the flow downstream the turbine for the frozen rotor and transient schemes.

According to this figure, the fluid reaches 80% of the free stream velocity at approximately 4 turbine diameters downstream of the frozen rotor configuration (approximately 48 m.) and approximately 3.8 turbine diameters downstream of the rotating blades configuration (approximately 45.6 m.). A 90% recovery is achieved however after the 86.4 m. downstream of the frozen rotor configuration and about 78 m for the transient configuration.

From the same figure, it can be deduced that when the turbines are of alignment in the Delta structure (23 m length), only a 66 % velocity recovery would be achieved according to the frozen rotor (brown dashed line of figure 6.19) whereas a 68 % velocity recovery would be achieved according to the transient (green dashed line of figure 6.19). This allows us to estimate the decrease of the efficiency of the turbine directly affected according to equations 4.2 and 4.3 as will be seen later.

Figure 6.20 shows the percentage of decrease in total pressure ratio, as a function of the yaw angle in a range from 0-30 degrees for all the configurations studied; such are the two porous media (9 and 10 m) and the other two unsteady models respectively. This ratio can be defined as the value of the pressure directly affected by the wake created for an upstream turbine over a downstream one of the Delta structure, divided by the mean operating pressure. For this case, longer values for this ratio have been reached for the two cases corresponding to the discrete blades models as apparently these models offer a notably lower resistance to the flow even for bigger yaw angles of the nacelles.

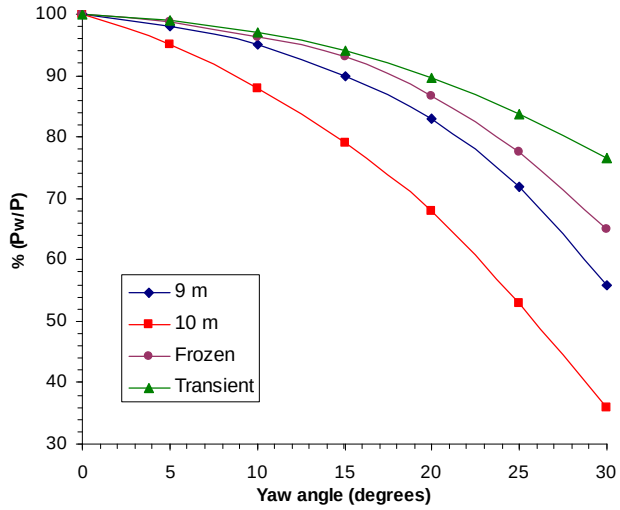

Figure 6.20. Pressure ratio (%) as a function of the yaw angle (degrees) for all the schemes.

Figure 6.21 shows the progress of the efficiency for all the models studied according to the yaw angle of the nacelles in a range from 0 to 30 degrees for the DIRECT configuration while figure 6.22 shows the same but for the REVERSE configuration. It can be observed that there is a slightly longer decrease of the efficiency in the DIRECT model, apparently because two front turbines are directly disturbing the flow over the downstream one while in the REVERSE configuration only one turbine is interacting with the flow of the downstream one.

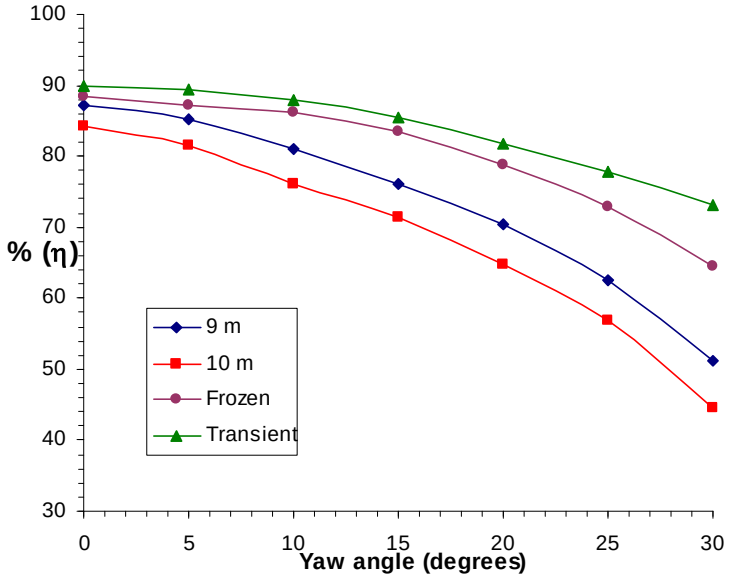

Figure 6.21. Efficiency (%) as a function of the yaw angle (degrees) for all the models (DIRECT).

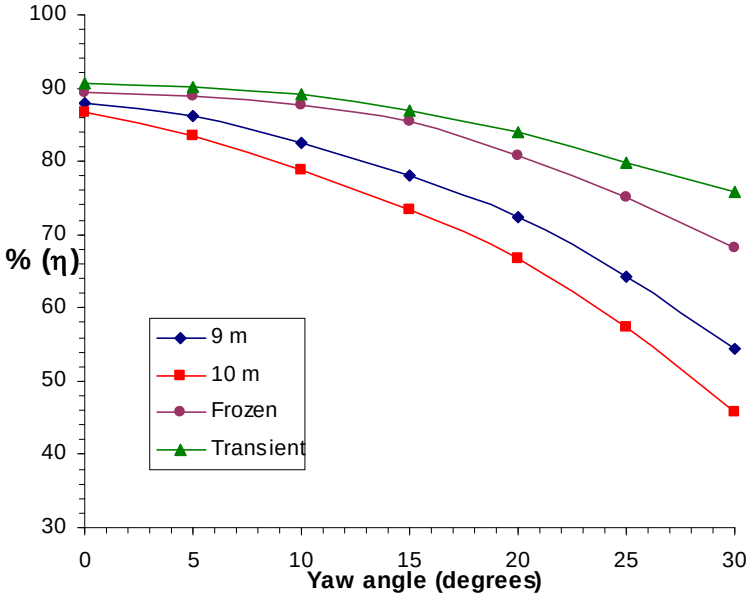

Figure 6.22. Efficiency (%) as a function of the yaw angle (degrees) for all the models (REVERSE).

7 VALIDATION OF THE MODELS

It is a strongly recommended practice to compare CFD results to other data sources in order to be able to validate properly the CFD model. These data can be obtained both in experimental or numerical ways, but also can be achieved through a literature review.

7.1 Experimental validation.

The validation of the transient CFD models has been realized through experimental velocity measurements over a 1/30 scale model in a water tank, carried out by the Off-shore Engineering and Naval Archicteture (OENA) Group of Cranfield University. Figure 7.1 shows the scale model used for both configurations.

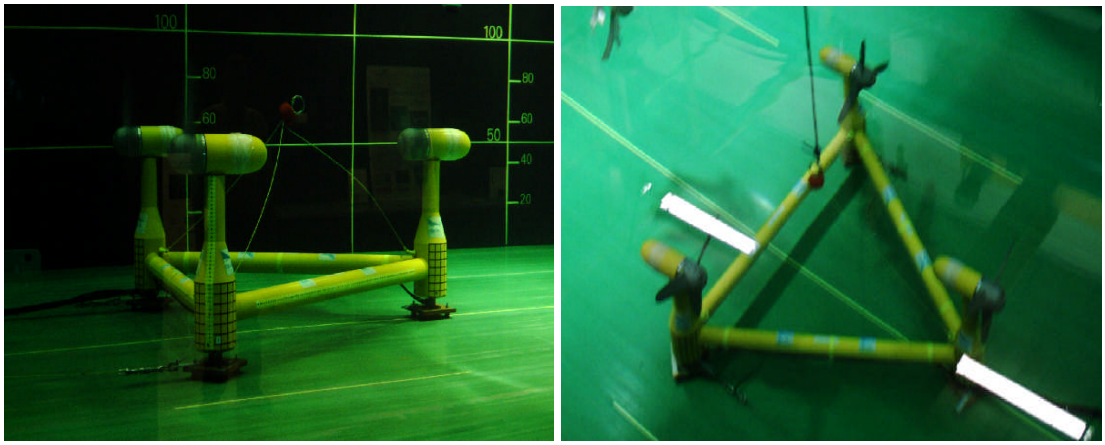

a **b**

Figure 7.1. Experimental scale model tested for both configurations DIRECT (a) and REVERSE (b).

Values for the velocity have been measured mainly downstream of the Delta configuration in vertical planes at a several normalised distances, according to figure 7.2 for validation purposes.

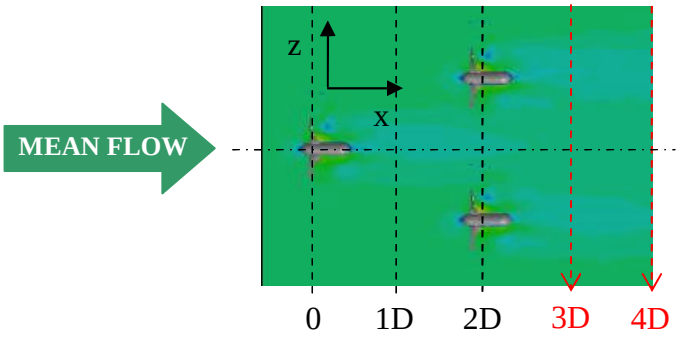

Figure 7.2. Assignment of the measurement planes for validation purpose.

In order to compare the results of the experimental model and the CFD, a non-dimensional study of the velocity can be seen in figure 7.3 where a comparative test showing the profiles of velocity at different vertical planes (mainly at 3D and 4D downstream respectively), as defined in last figure, was carried out. This figure shows the percentage of recovering velocity over the mean flow velocity. Dimensions are given once again in terms of disc diameters.

a

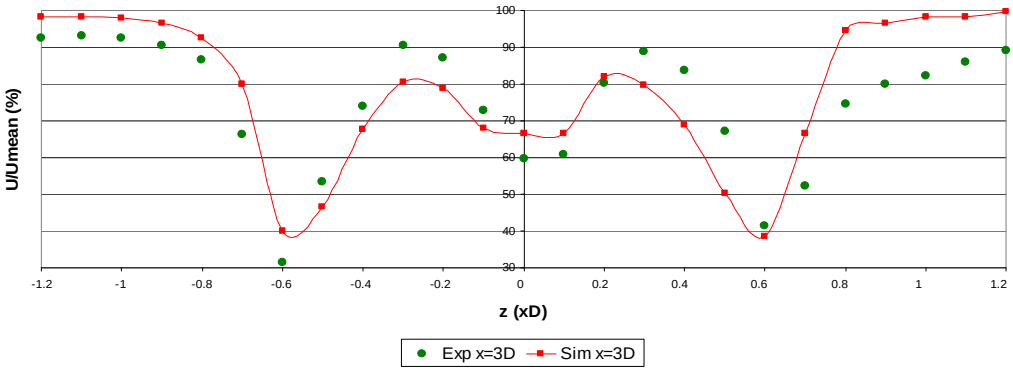

b

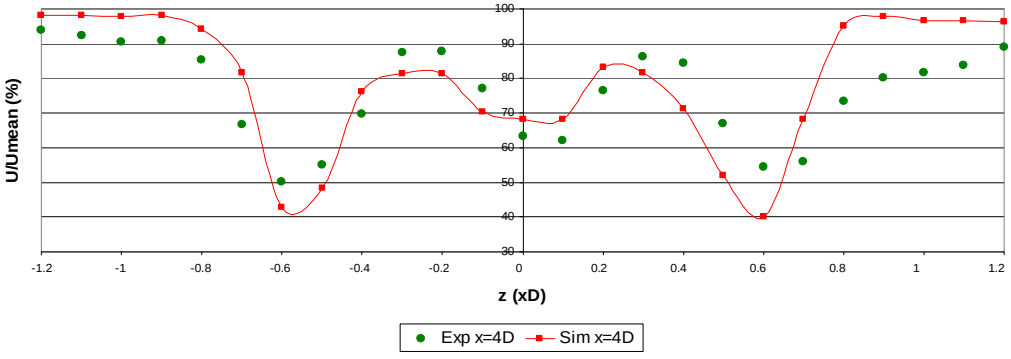

Figure 7.3. Non-dimensional velocity profiles at 3D plane (a) and at 4D plane (b) for experimental test and CFD simulations.

The mean (averaged) flow velocity for the experimental model was 0.6 m/s and for the CFD model 3.8 m/s, so velocity was also normalised. Results showed a good agreement between experimental data and CFD simulations.

Another way of validation for the transient CFD model is through a calculation from the experimental results by using MATLAB, also carried out by the OENA Group. This subroutine makes use of the experimental database provided, so related functions such are turbulent kinetic energy (TKE) or velocity fields can be depicted in the area surrounding the turbines. In figure 7.4, TKE contours through MATLAB (a) corresponding to the experimental model and the same from FLUENT® (b) corresponding to the CFD model, over a horizontal plane are depicted. Although they are not averaged, the main differences in value are of about 9 %.

a

b

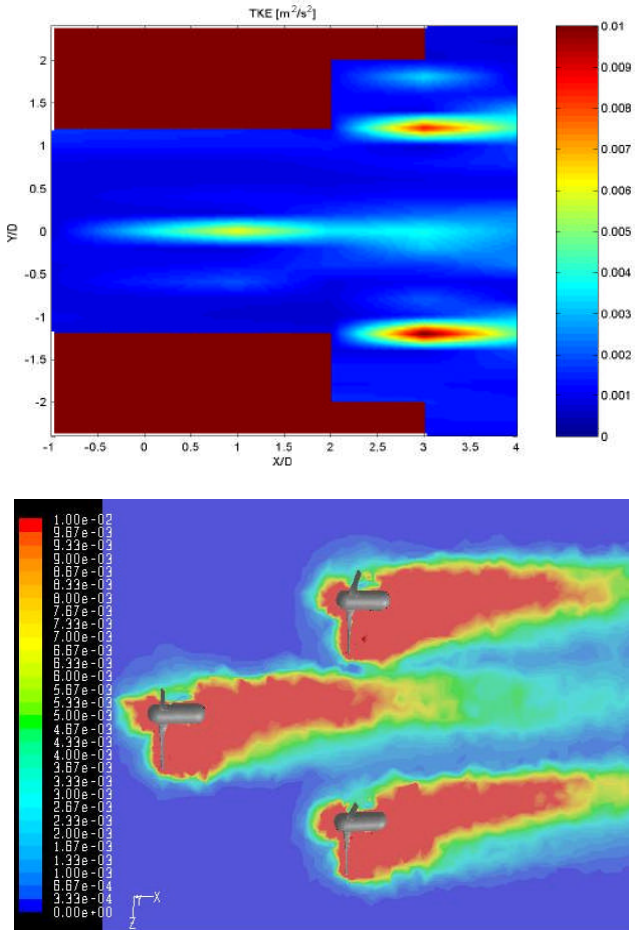

Figure 7.4. Turbulent Kinetic Energy contours (m^2s^2) through MATLAB (a) and CFD (b) over the horizontal plane of the nacelles.

7.2 Validation with the data from the literature.

Finally, according the results from Egarr et al (2004) [20] who plotted velocity magnitude of the fluid along a turbine axis both upstream and downstream, the gradual recovery of the velocity can be estimated. This is illustrated in Figure 7.5 together with the CFD results for the different models.

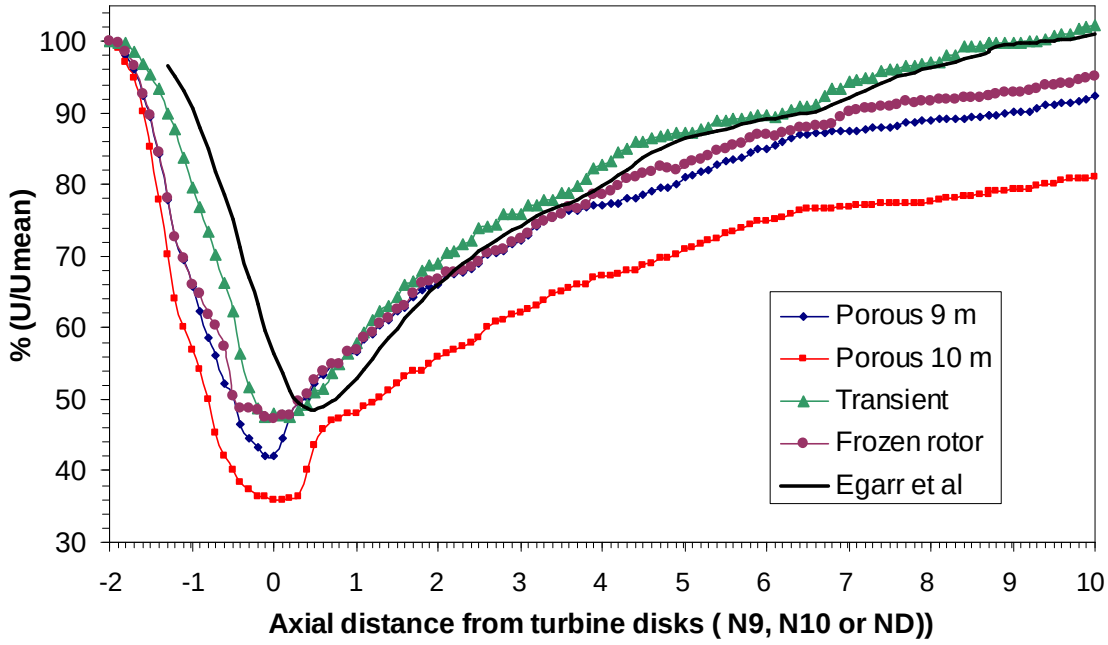

Figure 7.5. Validation of the CFD models through literature review.

It could be concluded, according to this figure that CFD models, especially the discrete blades models, are showing good agreement with the experimental results obtained from the literature. The best approach seems to be the transient model as it shows the closest results. On the contrary, the 10m porous media model offers the worst outputs as a longer resistance to the flow was achieved because the area occupied for the porous media itself is longer, considering the same resistance coefficient given for the two porous models.

8 CONCLUSIONS

The next conclusions derived from the work developed here can be summarised:

- CFD is a powerful tool which can provide precious information regarding the performance of such devices. This work presents the characterisation of the wake of a delta configuration for three horizontal axis marine current turbines through the use of this advanced computing facility. Understanding the lack of information about consequences of the interaction between these devices and the water flow, the study of the wakes has revealed as a significant concern in terms of improving the performance of the whole device.

- Wake characterisation around a single device was followed by the study of interaction effects between multiple turbines. It has been broadly probed that an increase in turbine yaw angle causes a considerable decrease of the power output [16]. The analysis of these results allowed a qualitative identification of the range of angular mismatch induced and the subsequent effect on the efficiency of the overall set of turbines. Several models have been taken into account in this work so the detailed conclusions achieved must be settled separately for each of them. The first of all is a porous media scheme which has been characterised, and modelled through different disc diameters, followed by a discrete blades representation which included as a first approach a frozen rotor model followed by a transient model.

- Regarding the porous media model, a turbulent model considering wall functions has been addressed in order to account for the flow through a porous medium. A faithful description of the structure has been modelled but porous discs have successfully been used to simulate the blades area, allowing investigation of the flow behaviour through them according to

the governing parameters selected. The coupled equations are successively solved using the SIMPLE algorithm. As expected, the porous insert successfully dampens the flow, greatly shrinking the recirculation zone. The effects are remarkable, either upstream or downstream. When the flow is fully turbulent, however, the amount of resistance to the flow offered by the porous region is obviously dependent on its width.

- There are several positions in which the interference due to front turbines could cause an excessive pressure drop to the downstream ones, depending on the configuration chosen, with the subsequent negative effect on its performance efficiency as has been demonstrated in figures 6.20 to 6.22. Special attention must be pointed out when considering alignment between turbines, which is the case of a yaw angle of 30 degrees for the nacelles, as can be seen in figure 6.18

- Apparently, figures 6.2 to 6.5, present an unusual increase in total pressure in the area surrounding the wakes as can be seen in the total pressure plots. This is probably due to a combination of the turbulent shear layer and the bounding free surface forcing a greater proportion of flow over the discs. Anyway this effect has been significantly decreased through the discrete blades models.

- With reference to the partially unsteady model (Frozen rotor), *SST k-ω* turbulence model has been considered as the best approach and preliminary results shows a good agreement with the porous media model both in average values but also in terms of wake profiles.

- Finally, regarding the full unsteady (transient), the main conclusion is that after a huge computational effort was needed, results show really good agreement with the experimental measurements carried out as can be deduced from figure 7.3.

- It can be concluded that CFD models presented can be considered validated through these experimental measurements carried out under the scope of this project. These experimental results were compared with the previous ones and validated through the data directly supplied through the experimental prototype but also through MATLAB calculations and finally through the literature review, as has been showed in figure 7.5.

- Finally, this thesis has successfully reviewed current state of the art regarding tidal extraction devices, focusing in horizontal axis machines so the author fulfilled the aim of this project, dealing with the flow behaviour through this particular configuration of marine device in order to evaluate the degree of angular mismatch that may occur between the three turbines of this device as the nacelles are yawed onto a range of angular settings.

9 FUTURE TASKS

Future work would be focused mainly on the improvement of the transient model, as this model has been demonstrated to be the best approach to the real scenario.

Besides, the improvement of the previous models in order to enhance the information related to the flow behaviour under different flow conditions would also be of interest. Thus, feasible future commitments to be made have been summarised in Table 9.1.

Model	Description of the task
POROUS MEDIA	- Improving boundary conditions for specific tidal devices. $\Delta P = f(u)$. - Considering different areas inside the discs with different boundary conditions.
TRANSIENT	- Continuing grid adaptation (refinement) surrounding the blades region. - Interactions with the flow (wakes) for different flow conditions. - Study of the wake effect on other neighbour delta configurations.

Table 9.1. Description of the future tasks for the porous media and transient models.

Due to the special character of the subject, which will lead indeed to innovative salient facts in the future, as has been clearly demonstrated through the literature, a further study would be focused mainly to improve results through other mesh adaptation processes (using velocity and/or pressure criteria) for all the models, specially for the last ones.

Other additional effort could be to extrapolate the methodology carried out here in order to analyze the interferences that may occur from one of these delta structures to other identical neighbour extraction devices in order to optimize the space in the sea bed among these tidal devices when thinking of settling a farm.

REFERENCES

[1] ETSU, *New and Renewable Energy: Prospects for the UK for the 21st Century - Supporting Analysis*, ETSU Report R-122, Harwell, Oxon, UK, 1999.

[2] Davis, B. V., Nova Energy Ltd. A Major Source of Energy from the Worlds Oceans, *IECEC-97 Conference*, Honolulu, July 31, 1997.

[3] Garwood (Jr.), R.W., Isakari, S.M. and Gallacher, P.C., *Thermobaric Convection, in, The Polar Oceans and Their Role in Shaping the Global Environment*, AGU Geophysical Monograph, 1994.

[4] Syri, S. The impacts of climate change mitigation on air pollutant emissions. In: Technology and climate change *CLIMTECH 1999–2002*. 14/2002 Final Report. Helsinki, Finland: The Finnish National Technology Agency (TEKES); 2002, 224-233.

[5] Mazumder R, Arima M. Tidal rhythms and their implications. *Earth-Science Rev* 2005; 69(1-2):79-95.

[6] O Rourke F. et al. Tidal energy update 2009. *Appl Energy* (2009), doi:10.1016/j.apenergy.2009.08.014

[7] Owen A, Trevor ML. Tidal current energy: origins and challenges. In: *Future energy*. Oxford: Elsevier; 2008. 111-28.

[8] Clarke J.A. et al. Regulating the output characteristics of tidal current power stations to facilitate better base load matching over the lunar cycle. *Renew Energy* 2006; 31(2):173-80.

[9] Boyle G. Renewable energy power for a sustainable future. 2nd ed. Berlin: Oxford University Press; 2004.

[10] Nicholls-Lee, R.F., Utilising Intelligent Materials in the Design of Tidal Turbine Blades. Poster Fluid and Structure Interactions Research Group, School of Engineering Sciences, University of Southampton, UK, 2008.

[11] Williams, G., Geological constraints on the Precambrian history of Earth's rotation and the Moon's orbit. *Reviews of Geophysics*, **38**, 2000. 37-60.

[12] Carbon Trust. *UK Tidal Stream Resource Assessment*. Produced by Black and Veatch Ltd., 2005.

[13] Munson, B. R., Young, D. F. and Okiishi, T. H., *Fundamentals of fluid mechanics*, 5th ed., John Wiley, NJ, 2006.

[14] Fraenkel, P.L., Power from marine currents, *J. Power and Energy*, 216 (1), 2002. 1-14.

[15] Hammons, T. J, Tidal Power, *Proceedings of the IEEE*, V. 8, N 3, pp. 121-139, March 1997.

[16] Nicholls-Lee, R.F., Turnock, S.R. and Boyd, S.W., Simulation based optimisation of marine current turbine blades. In, Betram, Volker and Rigo, Philippe (eds.) 7th International Conference on Computer and IT Applications in the Maritime Industries (COMPIT'08), Liège, 21-23 April 2008. Liège, Belgium, 314-328, 2008.

[17] Myers, L. and Bahaj, A.S., Simulated electrical power potential harnessed by marine current turbine arrays in the Alderney race, *J. Renewable Energy*, 30, 2005, 1713-1731.

[18] Blunden, L.S.; Bahaj, A.S., Initial evaluation of tidal stream energy resources at Portland Bill, UK, *J. Renewable Energy*, 31, 2006, 121-132.

[19] http://www.tidalenergyltd.com

[20] Egarr, D. A., O'Doherty, T., Morris, S. and Ayre, R. G., Feasibility Study Using Computational Fluid Dynamics for the Use of a Turbine for Extracting Energy from the Tide, *15th Australasian Fluid Mechanics Conference*, The University of Sydney, Sydney, Australia 13-17 December 2004.

[21] Blanco, J.M., Amaral, J., *Recent Patents on Tidal Power Extraction Devices*, Recent Patents on Engineering", 2009, V. 3, No. 3, 178-193.

[22] Blanco, J.M., Amaral, J. and Ayre, R., Investigation of Turbine Interaction in a Prototype "DeltaStream" Tidal Power Device, *Proceedings of the International Congress for Numerical Methods in Engineering*, Barcelona, Spain, 29 Jun -2 Jul 2009.

[23] Siddiqui, O. and Bedard, R., Feasibility assessment of offshore wave and tidal current power production: a collaborative public/private partnership, *IEEE Power Engineering Society General Meeting*, November 23-25, 2005.

[24] http://www.answers.com/topic/tidal-power

[25] Wikipedia, The Free Encyclopedia, "Tidal power". Wikimedia Foundation, Inc., 2008 <http://en.wikipedia.org/w/index.php?title=Tidal_power&oldid=228620488>

[26] Blunden, L.S.; Bahaj, A.S., Initial evaluation of tidal stream energy resources at Portland Bill, UK, *J. Renewable Energy*, 31, 2006. 121-132.

[27] http://www.emec.org.uk/marine_renewables.asp

[28] Germain, G, Bahag, A. S., Huxley-Reynard, C, Roberts, P., Facilities for marine current energy converter characterization, In: *Proceedings of the 7th European wave and tidal energy conference*, Porto, Portugal, 11-13 September 2007.

[29] Batten, W. M. J., Bahaj, A. S., Molland, A. F., Chaplin, J. R.**,** Hydrodynamics of marine current turbines, *J. Renewable Energy,* 31 (2), 2006. 294-256.

[30] Bahaj, A.S., Myers, L.E., Thomson M.D. and. Jorge, N., Characterising the wake of horizontal axis marine current turbines, *Proceedings of the 7th European wave and tidal energy conference*, Porto, Portugal, 11-13 September, 2007.

[31] Karsten, R. H, McMillan, J.M., Lickley, M.J. and Haynes, R. D., Assessment of tidal current energy in the Minas Passage, Bay of Fundy, *J. Power and Energy*, 2008, 494-507.

[32] Kirke, B., Developments in ducted water current turbines. Publication in: http://www.cyberiad.net/library/pdf/bk_tidal_paper25apr06.pdf

[33] Scheidegger, A. E., *The Physics of Flow through Porous Media*. University of Toronto Press, Toronto, 1974.

[34] Dewiest, R. J. M., *Flow through Porous Media*. Academic Press, New York, 1969.

[35] Vafai, K. and Tien, C.L., Boundary and inertia effects on flow and heat transfer in porous media, *Int. Journal of heat & Mass Transfer*, 24, 1981. 195-203.

[36] Borgesen, A.: EP1714027 **(2006).**

[37] Landberg, M.: EP1816345 **(2007).**

[38] Fraenkel, P. L.: EP1984572 **(2008).**

[39] Williams, H.: EP1878913 **(2008).**

[40] Masters, I., Orme, J.: EP2013474 **(2009).**

[41] Davis, B. V., Grillos, E., Allison, S.: WO2003025385 **(2003).**

[42] Mondl, F.: WO/2005/078276 **(2005).**

[43] Thothathri, K.: WO2007125538 **(2007).**

[44] Hill, E. A.: WO2008045662 **(2008).**

[45] Ganley, D. J.: WO2009049269 **(2009).**

[46] Stothers, R.: US20070284884 **(2007).**

[47] Ahdoot, N. M.: US20080260548 **(2008).**

[48] Jennings, C. A.: US20087470086 **(2008).**

[49] Devaney, T.: US20090015014 **(2009).**

[50] Nail, J. M.: US20090015018 **(2009).**

[51] Sternitzke, D. A.: US20097479708 **(2009).**

[52] Petrounevitch, E.: US20090026767 **(2009).**

[53] Costin, D. P.: US20097489046 **(2009).**

[54] Bernitsas, M. M., Raghavan, K.: US20097493759 **(2009).**

[55] Charlier RH. Forty candles for the Rance River TPP tides provide renewable and sustainable power generation. *Renew Sustain Energy* Rev 2007;11(9): 2032-57.

[56] Rourke FO, Boyle F, Reynolds A. Renewable energy resources and technologies applicable to Ireland. *Renewable and Sustainable Energy* Rev 2009;13(8):1975-84.

[57] Bryden IG, Grinsted T, Melville GT. Assessing the potential of a simple tidal channel to deliver useful energy. *Appl Ocean Res* 2004;26(5):198-204.

[58] Bryden IG et al. Matching tidal current plants to local flow conditions. *Energy* 1998;23(9):699-709.

[59] Kiho S, Shiono M, Suzuki K. The power generation from tidal currents by Darrieus turbine. *Renew Energy* 1996; 9(1-4):1242-5.

[60] Patankar, S., *Numerical heat transfer and fluid flow*, Hemisphere, Washington D.C., 1980.

[61] Feder, J., *Flow in porous media,* Lecture notes, Physics Dept., University of Oslo, Norway, 1995.

[62] Whitaker, S., Flow in Porous Media I: A Theoretical Derivation of Darcy's Law, *Transport in Porous Media,* 1, 1986. 3-25.

[63] Hassanizadeh, S. M., High velocity flow in porous media, *Transport in porous media*, 3. 1987. 521-531.

[64] Nield, A.D. and Bejan, A., Convection in Porous Media, Springer Verlag, N.Y., 1999.

[65] Whitaker, S.**,** Advances in theory of fluid motion in porous media, *Ind. Eng. Chem*. 61. 1969. 14-28.

[66] Menter, F.R., Eddy viscosity transport equations and their relation to the k-ε model. *J. Fluid Eng* 119, 1997. 876-884.

[67] Atta, A., Shantanu, R. and Nigam, K.D.P., Prediction of pressure drop and liquid holdup in trickle bed reactor using relative permeability concept in CFD, *Chemical Engineering Science*, 62, (21), 2007. 5870-5879.

[68] Choeng-Ryul, Ch, Tae-Soon K. and Chul-Hwa S., Numerical analysis and visualization experiment on behavior of borated water during MSLB with RCP running mode in an advanced reactor, *Nuclear Engineering and Design*, 237, 2007. 778–790.

[69] Fluent Inc (2006), Fluent 6.3 documentation.

[70] Lion W.W., Shabbir A. Shih, T.H. and Zhu, J., A new k-epsilon eddy-viscosity model for high Reynolds number turbulent flows - model development and validation, *Computers and Fluids*, 24 (3), 1995. 227-238.

[71] Wilcox, D.C., *Turbulence Modelling for CFD*, 2nd Edition. Griffin Printing, California, 1998.

[72] Menter, F. R., *Zonal Two Equation k-ω Turbulence Models for Aerodynamic Flows*, AIAA Paper 93-2906, 1993.

[73] Patankar, S. V. and Spalding, D.B., A calculation procedure for heat, mass and momentum transfer in three-dimensional parabolic flows. *International Journal of Heat and Mass Transfer*, 15, 1972, 456-473.

[74] Garwood (Jr.), R. W., Enhancements to deep turbulent entrainment, In: *Deep Convection and Deep Water Formation in the Ocean*, ed., by P.C. Chu and J.C. Gascard, Elsevier, 1991. 189-205.

[75] Perot, J. B., Are, S. and Zhang, X., Application of the turbulent potential model to unsteady flows and three-dimensional boundary layers, *Int. J. of Rotating Machinery*, 9 (5), 2003. 375-384.

[76] Menter, F. R. (1994), Two-Equation Eddy-Viscosity Turbulence Models for Engineering Applications, AIAA Journal, vol. 32, pp. 269-289, 1994.

BIBLIOGRAPHY

(In order of first author's name)

Journal articles

- Antohe, B.V., and Lage, J.L., A General Two-Equation Macroscopic Turbulence model for Incompressible Flow in Porous Media, *International Journal of Heat and Mass Transfer*, 40, 1997. 3013-3024.

- Bahaj, A. S. and Myers, L.E., Fundamentals applicable to the utilisation of marine current turbines for energy production, *J. Renewable Energy*, 28, 2003. 2205–2211.

- Bahaj, A. S., Molland, A. F., Chaplin, J. R., Batten, W. M. J., Power and thrust measurements of marine current turbines under various hydrodynamic flow conditions in a cavitation tunnel and a towing tank, *J. Renewable Energy*, 32 (3), 2007. 407-426.

- Bahaj, A. S., Batten, W.M.J., McCann, G., Experimental verifications of numerical predictions for the hydrodynamic performance of horizontal axis marine current turbines, *Renewable Energy* 32, 2007. 2479-2490.

- Batten, W.M.J., Bahaj, A.S., Molland, A.F., Chaplin, J.R., Experimentally validated numerical method for the hydrodynamic design of horizontal axis tidal turbines. *Ocean Eng*., 34 (7), 2007, 1013-29.

- Batten, W. M. J., Bahaj, A. S., Molland, A. F., Chaplin, J.R., Power and Thrust Measurements of Marine Current Turbines under various Hydrodynamic Flow Conditions in a Cavitation Tunnel and Towing Tank. *J. Renewable Energy*, 32 (3), 2007. 407-426.

- Blunden, L.S., Bahaj, A.S., Tidal energy resource assessment for tidal stream generators, *J Power Energy*; 221 (2), 2007. 137-46.

- Carsey, F. and Garwood (Jr.), R.W., *Geophys. Res. Lett*., 20, 1993. 2207-2210.

- Chwang, A.T., A porous wave maker theory. *Journal of Fluid Mechanics*, 132 (1), 1993. 395-406.

- Ebert, P.R. and Wood, D.H., The near wake of a model horizontal-axis wind turbine at runaway, *Renewable Energy*, 25, 2002. 41-54.

- Fraenkel, P., Marine currents: a promising large clean energy resource. *Power Generation by Renewables*, 2000. 221-234.

- Garrett, C. and Cummins, P. Generating power from tidal currents. *Ocean Eng.*, 130(3), 2004. 113-118.

- Gorban, A.N., Gorlov, A.M. and Silantyev, V.M., Limits of the turbine efficiency for free fluid flow, *Journal of Energy resources technology*, 123, 2001. 311-317.

- Khan, M.J., Bhuyan, G., Iqbal, M.T. and Quaicoe, J.E., Hydrokinetic energy conversion systems and assessment of horizontal and vertical axis turbines for river and tidal applications: A technology status review, *Applied Energy*, 86, 2009. 1823-1835.

- Launder, B.E., and Spalding, D.B., The Numerical computation of Turbulent Flows, *Computer Methods in Applied Mechanics and Engineering*, 3, 1974. 269-289.

- Lawn, C.J., Optimization of the power output from ducted turbines, *Journal of Power and Energy*, vol. 217, no. 1, 2003. 107-117.

- Myers, L. and Bahaj, A. S. Power output performance characteristics of a horizontal axis marine current turbine, *Renewable energy*, 31, 2006. 197-208.

- Myers, L. and Bahaj, A.S., Wake studies of a 1/30th scale horizontal axis marine current turbine, *Ocean Engineering*, 34, 2007. 758-762.

- Perot, B.J. and Chang, W. 2002, Prediction of turbulent transition in boundary layers using the turbulent potential model, *J. Turbulence*, 3 (22), 2002. 1-15.

- Ullman, P.W., Offshore tidal power generation A new approach to power conversion of the oceans' tides, *MTS Journal*, 36 (4), 2002. 16-24.

Conference papers

- Barltrop, N., Varyani, K S, Grant, A, Clelland, D. and Pham, X.P., Wave-current interactions in marine current turbines, In: *Proceedings of the Institution of Mechanical Engineers*, Part M: Journal of Engineering for the Maritime Environment, Volume 220, Number 4, 2006.

- Barltrop, N., Varyani, K S, Grant, A, Clelland, D. and Pham, X.P., Investigation into wave-current interactions in marine current turbines, In: *Proceedings of the Institution of Mechanical Engineers*, Part A: Journal Power and Energy, Volume 221, 2007.

- Batten, W.M.J., Bahaj, A.S, Molland, A.F. and Chaplin, J.R., Experimentally validated numerical method for the hydrodynamic design of horizontal axis tidal turbines. In: *Proceedings of sixth European wave and tidal energy conference*, Glasgow, 29th Sept–2nd Oct 2005.

- Bryden, I. and Melville, G T, Choosing and evaluating sites for tidal current development, In: *Proceedings of the Institution of Mechanical Engineers,*. Vol. 218 Part A, 2004.

- Bryden, I., Couch, S.J., Owen, A. and Melville, G T, Tidal current resource assessment, In: *Proceedings of the Institution of Mechanical Engineers*. Vol. 218 Part A, 2004.

- Blunden, L. S. and Bahaj, A. S. Comparison of different approaches to site selection for tidal stream energy resource assessment. In: *Second International Conference on Renewable energy in maritime island climates*, Dublin, Ireland, 26–28 April 2006.

- Campos, F.; Weston, S.; Schumacher, T., Automatic optimisation of CFD engineered designs, Automated Design & Optimisation Techniques using CFD, In: *IMechE*, 2006, London.

- Cave, P. R., Evans, E. M., and George, K. J. Assessment of tidal streams as an energy resource. In: *Fifth International Conference on Energy options - the role of*

alternatives in the world energy scene, University of Reading, UK, 1987, pp. 153–156 (IEE, London).

- Child, B. F. M. and Venugopal, V., Interaction of waves with an array of floating wave energy devices, In: *Proceedings of the 7th European wave and tidal energy conference*, Porto, Portugal, 11-13 September 2007.

- Clarke, J. A., Grant, A. D. and Johnstone, C.M., Output Characteristics of Tidal Current Power Stations, In: *Proceedings of The Fourteenth International Offshore and Polar Engineering Conference*, Toulon, France, May 23-28, 2004

- Clarke, J. A., Connor, G., Grant, A. D., Johnstone, C. M. and Mackenzie, D., Design and initial testing of a contra-rotating tidal current turbine. In: *Proceedings of the World Renewable Energy Congress*, 19 -25 August, 2006, Florence, Italy.

- Clarke, J.A., Connor, G., Grant, A. D., Johnstone, C. M. and Mackenzie, D., Development of a Contra-Rotating Tidal Current Turbine and Analysis of Performance, In: *Proceedings of the 7th European Wave and Tidal Energy Conference*, Porto, Portugal, 2007.

- Couch, S.J., Bryden, I., Tidal Current Energy Extraction: Hydrodynamic Resource Characteristics, In: *Proceedings of the Institution of Mechanical Engineers*, Part M: Engineering for the Maritime Environment, pp 185-194, 2006.

- Eça, L, and Hoekstra, M., An evaluation of verification procedures for CFD applications. In: *Proceedings of the 24th symposium on naval hydrodynamics*, Fukuoka, Japan, 8-13 July 2002.

- Fraenkel, P.L., Clutterbuck, P., Stjernstrom, B. and Bard, J. Tidal and Marine Currents, In: *Proceedings of the 3rd European Wave Energy Conference,* , Patras, Greece, 30th September - 2nd October 1998.

- Gorlov, A.M., The Helical Turbine and its applications for tidal and wave power, In: *Proceedings of IEEE OCEANCS'03*, vol. 4, San Diego (USA), September 2003.

- Hammons, T.J., Tidal power, In: *Proceedings of the. IEEE*, V 3, N 8, pp. 419-433, March 1993.

- Isakari, S.M. and Garwood (Jr.), R.W., Deep free convection in the Greenland and Mediterranean Seas, Poster and Video In: *Third Scientific Meeting of the Oceanography Society*, Seattle, April 13- 16, p. 184, 1993.

- Jones, A.T. and Westwood, A., Recent Progress in Offshore Renewable Energy Technology Development, In: *Proceedings of IEEE PESGM'05*, vol. 2, pp 2017-2022, San Francisco(USA), June 2005.

- Kerbiriou, M.A., Prevosto1, M., Maisondieu, C., Clément, A., Babarit, A., Influence of Sea-States Description on Wave Energy Production Assessment, In: *Proc 7th European Wave and Tidal Energy Conference*, Porto, Portugal, 11-13 September 2007.

- Lendenmann, H., Strømsem, K. C., Dai Pre, M., Arshad, W., Leirbukt, A., Tjensvoll, G. and Gulli, T., Direct generation wave energy converters for optimized electrical power production, In: *Proceedings of the 7th European wave and tidal energy conference*, Porto, Portugal, 11-13 September 2007.

- Macleod, A., Barnes, S., Rados, K. G. and Bryden, I. G., Wake effects in tidal current turbine farms. In: *Proceedings of MAREC 2002*, University of Newcastle, 2002.

- Melville, G. T., Rados, K. and Bryden, I. G. Model to optimise the electrical and economic performance of tidal current energy conversion systems. In: *Proceedings of MAREC 2001*, University of Newcastle, 2001.

- Molland, A. F., Bahaj, A. S., Chaplin, J. R., Batten, W. M. J., Measurements and predictions of forces, pressures and cavitations on 2-D sections suitable for marine current turbines, In: *Proc. IMechE*, 218, pp.127-138, 2004.

- Myers, L. and Bahaj, A. S. Basic operational parameters of a horizontal axis marine current turbine. In: *Proceedings of Eighth World Renewable Energy Congress*, Denver, USA, 2004.

- Nicholls-Lee, R.F., Utilising Intelligent Materials in the Design of Tidal Turbine Blades. Poster Fluid and Structure Interactions Research Group, UK, In: *Proceedings of the Oceans'07, IEEE,* Aberdeen, 2007.

- Nicholls-Lee, R.F., Adaptive Composite Blades for Improved Performance of Horizontal Axis Tidal Turbines, Poster, Fluid and Structure Interactions Research Group, UK, In: *Proceedings of the Oceans'07, IEEE,* Aberdeen, 2007.

- Nicholls-Lee, R.; Turnock, S. R., Enhancing performance of a horizontal axis tidal turbine using adaptive blades, In: *Proceedings of the Oceans'07, IEEE,* Aberdeen, 2007.

- Norris, J.V., E. Droniou, E., Update on EMEC activities, resource description, and characterisation of wave-induced velocities in a tidal flow. In: *Proc 7th European Wave and Tidal Energy Conference*, Porto, Portugal, 11-13 September 2007.

- Polinder, H., Mueller, M. A., Scuotto, M. and Goden de Sousa Prado, M., Linear generator systems for wave energy conversion, In: *Proceedings of the 7th European wave and tidal energy conference*, Porto, Portugal, 11-13 September 2007.

- Raven, H.C., Van der Ploeg, A, and Eça, L., Extending the benefit of CFD tools in ship design and performance prediction. In: *Proceedings of the 7th international conference on hydrodynamics*, Ischia, Italy. October 4-6, 2006.

- Redford, J. A. and Johnson, M. W., Predicting transitional separation bubbles, In: *Proceedings of TURBOEXPO: International Gas Turbine Congress*, Vienna, Austria, 2004.

- Trapp, T., Developing and building the Stingray tidal stream generator. In *Proceedings of MAREC 2002*, University of Newcastle, 2002.

- Wang, D.; Atlar, M., Experimental investigation on cavitation performance, noise characteristics and slipstream wash of an ocean stream turbine, In: *World Maritime Technology Conference, IMarEST*, London, 2006.

- Ward, J.C., Turbulent Flow in Porous Media, In: *Proceeding of the ASCE Journal of Hydraulics*, 90, HY5, 1964. 1-12.

- Whelan, J., Thomson, M. Graham, J. M. R. and Peiró, J., Modelling of free surface proximity and wave induced velocities around a horizontal axis tidal stream turbine, In: *Proceedings of the 7th European Wave and Tidal Energy Conference*, Porto, Portugal, 11-13 September 2007.

Books, reports and other publications

- Bahaj, A.S., Batten, W.M.J., Molland, A.F., Chaplin, J.R., *Theoretical predictions of the hydrodynamic performance of marine current turbines*. Sustainable energy series, Report 4, University of Southampton, March 2005.
- Bedard, R., Previsic, M., Polagye, B. and Casavant, A. *A Feasibility Study of* In Stream Tidal Energy Conversion *Technology in North America*, EPRI TP-008-NA, 2006.
- Black & Veatch, *UK Tidal Stream Energy Resource and Technology*. Summary Report for the Carbon Trust, 2005.
- Boyle, G., *Renewable energy: power for a sustainable future*, Oxford University press, 2009.
- Carbon Trust, *Variability of UK marine resources, produced by Environmental Change*, Institute, Oxford, 2005.
- Chandrasekhara, B. C. and Vortmeyer, D., *Flow mode1 for velocity distribution in fixed porous beds under isothermal conditions*, Thermo- and Fluid Dynamics 12105-12111, 1979.
- Charlier R.H., *Tidal Energy*. New York: Van Nostrand Reinhold, 1982.
- Christopher, D.M., *Heat Transfer in Porous Media and Particulate Flows*, ASME Publication HTD 46, 1985.
- Collins, R. E., *Flow of Fluids through Porous Materials*. Reinhold, New York, 1961.

- Couch, S. J., *Numerical modelling of tidal flows around headlands and islands*. PhD Thesis, University of Strathclyde, T10342, 2001.

- DTI report, *Development, installation and testing of a large scale tidal current turbine*, Contract number T/06/0021/00/Rep, October 2005.

- European Commission, *The Exploitation of Tidal Marine currents*, Report EUR16683EN, 1996.

- Fraenkel, P.L. *Tidal currents A major new source of energy for the Millennium* EEZ Technology. 4th ed. London: ICG Publishing Ltd, 1999.

- Fraenkel, P.L., *Marine Current Turbines: an emerging technology*, Paper for Scottish Hydraulics Study Group Seminar in Glasgow on 19 March 2004.

- Fraenkel, P.L., *Tidal Current Energy Technologies*, Ibis, Volume 148, Supplement 1, March 2006 , pp. 145-151(7), Blackwell Publishing, 2006.

- Frisch, U., *Turbulence*. Cambridge: Cambridge University Press, 1995.

- Gunzburger, M.D., *Finite Element Methods for Viscous Incompressible Flows: A guide to theory, practice, and algorithms*, Academic Press, Inc. 1989.

- Hunt, J.C.R., Phillips, O.M. and Williams, D., *Turbulence and Stochastic Processes; Kolmogoroff 's Ideas 50 years On*. London: The Royal Society, 1991.

- Jonsson, I. G., *Wave-Current Interactions, Ocean Engineering Science*, In: The Sea, Volume 9, Part A, Chapter 3, 1990.

- Kundu, P. K. and Cohen, I. M., *Fluid mechanics*, 4th ed, Academic Press, London, 2007.

- Mei, C., *The Applied Dynamics of Ocean Surface Waves*, World Scientific Publishing Co. Pte. Ltd., London, 1989.

- UK Department of Energy, *Offshore Installations, Guidance on Design, construction and Certification*, HMSO, London, Fourth Edition, 1990.

- UK DTI, *Marine Renewables Wave and Tidal-stream Energy Demonstration Scheme*, May 2005.
- Wang, D., Atlar, M., and Paterson, I. *Performance tests of the third tidal stream rotor*. Report No. MT2005-002, School of Marine Science and Technology, University of Newcastle upon Tyne, January 2005.
- White, F.M., *Fluid mechanics*, Third Edition, McGraw Hill, 1979.

Internet sources

- http://www.bluenergy.com/tidal.html
- http://congress.cimne.com/metnum09/frontal/default.asp
- http://www.cyberiad.net/library/pdf/bk_tidal_paper25apr06.pdf
- http://www.dti.gov.uk/files/file23963.pdf
- http://www.europeanenergyventurefair.com
- http://www.eu-oea.com/index.asp?bid=232
- http://www.fluentusers.com
- http://www.iht.com/articles/2002/08/26/rwave_ed3_.php
- http://www.imeche.org/about/keythemes/energy/Energy+Supply/Renewable+energy/Marine+Energy/Tidal+power/
- http://www.itpower.co.uk/Technologies/Ocean_Energy
- http://www.marineturbines.com
- http://www.openhydro.com/home.html
- http://www.tidalgeneration.co.uk
- http://kn.theiet.org/magazine/issues/0816/tidal-0816.cfm

- http://www.worldenergy.org/publications/survey_of_energy_resources_2007/tidal_energy/755.asp
- http://www.uspto.gov
- http://ep.espacenet.com/
- http://www.freepatentsonline.com/
- http://www.google.com/patents
- http://patft.uspto.gov/netahtml/PTO/search-bool.

****END OF THESIS***